

# Recent Advances in Aerobic Oxidation of Alcohols and Amines to Imines

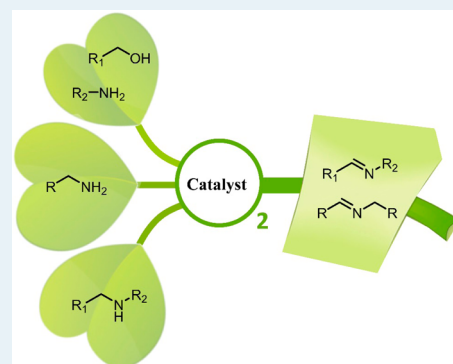
Bo Chen,<sup>†,‡</sup> Lianyue Wang,<sup>†</sup> and Shuang Gao<sup>\*,†</sup>

<sup>†</sup>Dalian Institute of Chemical Physics, Chinese Academy of Sciences, Dalian National Laboratory for Clean Energy, Dalian 116023, China

<sup>‡</sup>University of the Chinese Academy of Sciences, Beijing 100049, China

**ABSTRACT:** Imines as valuable intermediates are widely applied in pharmaceutical syntheses and organic transformation. However, the traditional imine synthesis involves unstable aldehydes, dehydrating agents, and Lewis acid catalysts. The topic of this review is focused on three new approaches, namely, the cross-coupling of alcohols with amines, the self-coupling of primary amines, and the oxidative dehydrogenation of secondary amines, utilizing much more readily available starting materials and green oxidant ( $O_2$ /air) to furnish the imine products. The related catalysts are classified into metal, metal-free, photo-, and bioinspired catalysts. Particular emphasis is placed on the high-activity, low-cost, and versatile catalysts; key factors that affect the catalytic activity and reaction mechanisms are also highlighted.

**KEYWORDS:** aerobic oxidation, alcohols, amines, catalysis, imines



## 1. INTRODUCTION

Imines, also known as Schiff bases, are versatile intermediates for the synthesis of pharmaceutically and biologically active compounds, and fine chemicals.<sup>1</sup> The C=N bond in imines is also widely used in organic transformations such as reduction, addition, cyclization, and aziridination reactions.<sup>2</sup> Traditionally, imines are prepared by the condensation of amines with carbonyl compounds, especially unstable aldehydes, and dehydrating agents as well as Lewis acid catalysts are required in many situations.<sup>3</sup>

During the past decade, considerable efforts have been devoted to the direct synthesis of imines, in particular via one-pot procedures through an oxidative process to reduce the energy consumption, waste emission, operating and purification steps.<sup>4</sup> Among the various methodologies for imine formation, the following three approaches have received much more attention and have been greatly studied because the starting materials are readily available, and green molecular oxygen or air can serve as the terminal oxidant. (1) The cross-coupling of alcohols with amines (Scheme 1a): the only byproduct is water, and diverse symmetric and unsymmetric imines can be easily synthesized choosing different starting substrates. Nevertheless, the selective oxidation of alcohols into aldehyde intermediates under mild conditions remains the major challenge for this type of reaction.<sup>5</sup> (2) The self-coupling of primary amines (Scheme 1b): NH-imines generated from the dehydrogenation of primary amines or aldehydes formed by further hydrolysis of the NH-imines are generally proposed as the key intermediates. Homocoupled imines are facilely obtained via this process, whereas heterocoupled imines are much less accessible due to the

intrinsic self-coupling properties of the substrates. Besides, primary amines may also be transformed into nitrile, amide, azo compound byproducts. (3) The oxidative dehydrogenation of secondary amines (Scheme 1c): high selectivity is readily achieved because the substrates cannot be dehydrogenated into nitriles, and the products, such as cyclic imines, are usually very stable. However, the efficiency of the substrate conversion is influenced by the steric hindrance around the N-H, and the chemoselectivity for the oxidation of unsymmetric dibenzylamines is often blocked by the two types of  $\alpha$ -CH which possess similar properties but produce different products.

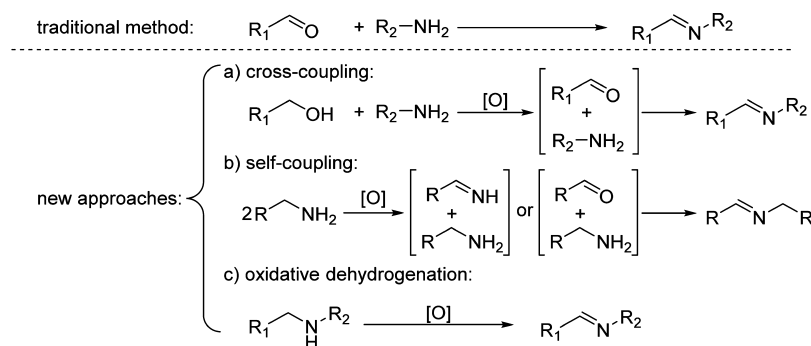
Aiming at the challenges, a wide variety of catalysts have been extensively explored during the past years and bring significant developments to these three new approaches. In this review, we seek to outline these fruitful achievements that have been made since 2009. Four group catalysts, metal, metal-free, photo-, and bioinspired catalysts, classified by their inherent features rather than by the reactions, will be discussed; this is possible because alcohol and amine substrates have similar physicochemical properties and share the same intermediates in many reactions. Particular emphasis will be placed on the high-active, low-cost, and versatile catalysts as they make the imine formation more practical and efficient; key factors that affect the catalytic activity and reaction mechanisms will also be highlighted, both of which are beneficial for designing new catalysts.

**Received:** July 14, 2015

**Revised:** August 24, 2015

**Published:** August 26, 2015

**Scheme 1. Imine Formation via Traditional Method and New Approaches by Aerobic Oxidation of Alcohols and Amines (a, b, and c)**



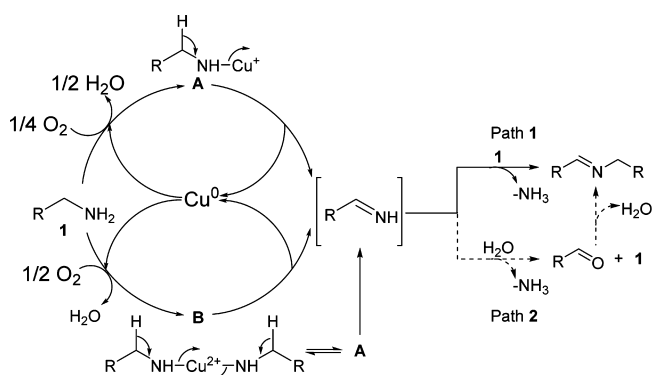
## 2. METAL-BASED CATALYSTS

Metal-catalyzed imine formation can be roughly classified into non-noble and noble catalysts. In terms of the oxidants, most metal-involved reactions are performed using dioxygen as the terminal oxidant, but a few noble metal complexes, such as Ir, Rh, and Ru, can promote the direct dehydrogenation of alcohols or amines under inert atmosphere.<sup>6</sup> Although it can avoid the possible problems of overoxidation under aerobic conditions, the dehydrogenation without additional oxidant often leads to the hydrogenation of imine products with the in situ formed metal-hydrides to form secondary amine byproducts through a “borrowing-hydrogen” process.<sup>7</sup> Besides, the toxicity, price, and stability as well as harsh reaction conditions also prohibit the practical applications of these catalysts. Thus, noble-metal-complex-catalyzed dehydrogenation methods under inert atmosphere are not covered here. On the other hand, given the fact that the main active sites of some non-noble metal catalysts are not the metals themselves but the additives such as ligands and linkers, inorganic base-mediated imines synthesis will be discussed in this part.

**Cu Catalysts.** In 2011, Patil et al. reported a concise method for imine formation by employing CuCl at 100 °C under neat conditions.<sup>8</sup> High activity was observed for the oxidation of various primary benzylic and cyclic amines, whereas the selectivity was hindered by the residual aldehydes (5–22%). Subsequently, they overcame the issue choosing copper powder instead of copper salt as the catalyst, and the yields were up to 90% under similar conditions.<sup>9</sup> Meanwhile, they found that the moisture in air played crucial roles in both promoting the reaction and avoiding the amine overoxidation, as poor selectivity was observed performing the reaction under pure oxygen atmosphere. The reaction mechanism was proposed as follows (Scheme 2): the initial oxidative addition of amine substrates to the copper powder with the assistance of O<sub>2</sub> would result in the formation of copper–amine complexes A and B; subsequent reductive elimination of these complexes would release NH-imine intermediates, which can either directly react with, or hydrolyze into aldehydes and further condense with, the substrates to produce imine products. Because no aldehyde was observed during the reaction, the direct addition may be favored in this catalytic system.

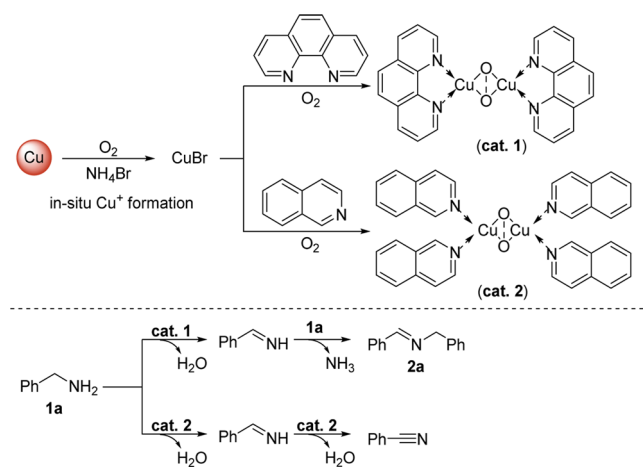
Inspired by the active species that can be generated in situ, Gu et al. combined organic ligands with red copper to fabricate more active catalysts.<sup>10</sup> The roughened surface observed from scanning electron microscopy (SEM) indicated that the red copper was partially oxidized into Cu<sub>2</sub>O under oxygen atmosphere, and further reacted in situ with NH<sub>4</sub>Br additive to

**Scheme 2. Proposed Mechanism for Copper-Catalyzed Self-Coupling of Primary Amines**



produce CuBr. Subsequent coordination with organic ligands and addition of oxygen led to transformation of CuBr into the activated Cu–oxygen complexes (Scheme 3). Interestingly, the

**Scheme 3. Proposed Mechanism for Amine Oxidation by Copper Complexes**



final products can be switched by the organic ligands: imines were obtained in the presence of 1,10-phenanthroline, whereas nitriles were generated utilizing isoquinoline under the same conditions.

In addition to amine oxidation, copper complexes have also been explored in cross-coupling of alcohols with amines. Zhang et al. found that copper(II) salts generally showed better selectivity than copper(I) salts, and benzyl alcohol can be

smoothly coupled with various aromatic or aliphatic amines to give the desired imines in good yields.<sup>11</sup> However, the requirement of stoichiometric KOH made the reaction less attractive. The same reaction was also examined using a dicopper(I) complex  $(\text{Cu}_2(\text{bnpn})(\mu\text{-OH})(\text{HCOO})_3)$ ; bnpn: 2,7-bis(2-pyridyl)-1,8-naphthyridine.<sup>12</sup> Although the amount of  $\text{CsOH}\cdot\text{H}_2\text{O}$  was decreased to 50 mol %, elevated temperatures and narrow alcohol scopes still limited the final application of the catalyst.

To overcome the above drawbacks and improve the catalytic efficiency of copper-based systems, additional additives were greatly explored over the past years, and nitroxyl derivatives were proposed as the most efficient cocatalysts. In 2012, Kerton et al. first reported a  $\text{CuBr}_2/2,2,6,6\text{-tetramethylpiperdinyl-N-oxyl}$  (TEMPO)-mediated imine formation from primary amines.<sup>13</sup> Unlike the simple  $\text{CuCl}$  system,<sup>8</sup> the reaction here can be performed at room temperature, and no residual aldehydes were detected during the reaction. Besides, the electronic properties of the substrates have no effect on the efficiency of the catalyst. A different mechanism was thus proposed: the intermediate **B** formed by the coordination of benzylamine to the  $\text{Cu(II)}$  complex **A** can further combine with TEMPO to form the key species **C**; after the C–H abstraction by the coordinated TEMPO, **C** was transformed into the radical intermediate **D**, which can be stabilized by the hydrogen bond between the second  $\beta$ -hydrogen atom and the oxygen atom of TEMPO-H; then, the NH-imine and TEMPO-H were dissociated from **D** via a single proton transfer, and the former was condensed with a free substrate to produce the desired imine, while the latter was oxidized by  $\text{O}_2$  to give TEMPO; finally, **A** was regenerated from the reduced  $\text{Cu(I)}$  complex **E** with the assistance of TEMPO (Scheme 4). Notably, this catalytic system was not only suitable

and long reaction times (60 °C, 48–60 h), but for primary amine oxidation, nitrile byproducts (2–23%) were detected in many situations.<sup>14</sup>

Kanai et al. developed another different catalytic system with ketoABNO rather than TEMPO as the cocatalyst.<sup>15</sup> Benefiting from the less steric profile and electron-deficient feature of ketoABNO, the  $\text{CuBr}/\text{ketoABNO}$  was found to be very active in both the primary and secondary amine oxidation under mild conditions (Scheme 5). For example,  $\alpha$ -methylbenzylamine, inactive in the  $\text{Cu}/\text{TEMPO}$  system, was smoothly transformed into the desired imine in 89% yield.

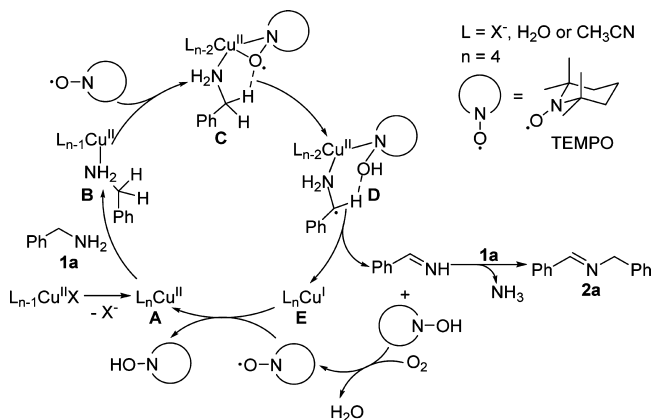
Given the high activity toward alcohol oxidation,  $\text{CuBr}/\text{nitroxyl}$  catalysts are also competent for the formation of heterocoupled imines from alcohols and amines.<sup>16</sup> In 2012, Xu et al. reported a  $\text{CuI}/\text{TEMPO}/2,2'\text{-bipyridine}$  (bipy) system for the cross-coupling of alcohols with amines at room temperature under base-free conditions.<sup>17</sup> Benzyl, allyl, propargyl, and even aliphatic alcohols were suitable for the reaction. As for the amine part, aliphatic amines and benzylamines were more active than anilines (Scheme 6). Besides, it should be mentioned that amine substrates worked not only as coupling reagents in the synthesis of imine products but also as promoters to facilitate the alcohol oxidation.

Following this work, Zhao et al. evaluated various ligands on the efficiency of  $\text{Cu}(\text{OAc})_2/\text{TEMPO}$ .<sup>18</sup> Simple 4-dimethylaminopyridine (DMAP) turned out to be the best ligand for alcohol oxidation, while bipy, consistent with the results of Xu,<sup>17</sup> was inefficient in the absence of amines. Applying this  $\text{Cu}(\text{OAc})_2/\text{TEMPO}/\text{DMAP}$  in the cross-coupling of benzyl alcohols with anilines or aliphatic amines, good to excellent yields were obtained at 110 °C and under solvent-free conditions. Moreover, a 100 g-scale of imine formation with 91% yield can be achieved with 0.5 mol % catalyst in 36 h, which highlighted the power as well as the practical application of this catalyst.

Despite the great exploration in homogeneous systems, Cu-based heterogeneous catalysts were really scarce. In 2013, Jones et al. studied the catalytic behavior of  $\text{CuO}/\text{CeO}_2$  for the self-coupling of benzylamine.<sup>19</sup> It was demonstrated that  $\text{CeO}_2$  can promote the generation of NH-imine intermediate by activating the N–H bond of benzylamine and adsorbing the formed water, but on the other hand, it may lead to the decomposition of imine products at prolonged reaction times. A leaching test disclosed that the catalysis was primarily associated with turnover by soluble copper species, and the reaction rate was increased in proportion to the amount of these soluble species. Although both  $\text{CuO}$  and  $\text{CeO}_2$  alone were active,  $\text{CuO}/\text{CeO}_2$  was shown to most efficiently catalyze the reaction. Kinetic experiments further revealed that the reaction promoted by the two metal oxides via different pathways, but NH-imine was proposed as the common intermediate: in the presence of  $\text{CuO}$ , the intermediate was directly coupled with free benzylamine to give the corresponding imine; whereas, it would be hydrolyzed into benzaldehyde and subsequently condensed with the substrate using  $\text{CeO}_2$  as the catalyst. Thus,  $\text{CuO}/\text{CeO}_2$  containing the above two pathways was more active than individual  $\text{CuO}$  and  $\text{CeO}_2$ .

Ramón et al. utilized  $\text{CuO}/\text{Fe}_3\text{O}_4$  to directly synthesize aromatic imines.<sup>20</sup> The reactions, however, were performed under an inert atmosphere, and stoichiometric  $\text{NaOH}$  was added in both the self-coupling of amines and cross-coupling of alcohol with amines. Besides, it should be pointed out that the presence of nitrogen-containing compounds can increase the particle size of  $\text{CuO}$  and promote the copper leaching by formation of copper complexes. Thus, considerable loss of activity was observed in

**Scheme 4. Proposed Mechanism for  $\text{CuBr}_2/\text{TEMPO}$ -Catalyzed Oxidation of Benzyl Amines<sup>a</sup>**

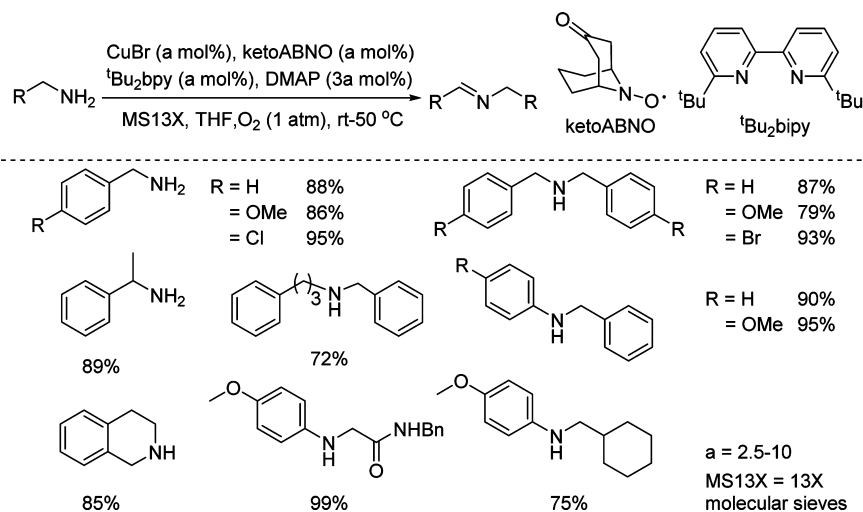


<sup>a</sup>The loss and coordination of L throughout the cycle were omitted for clarity.

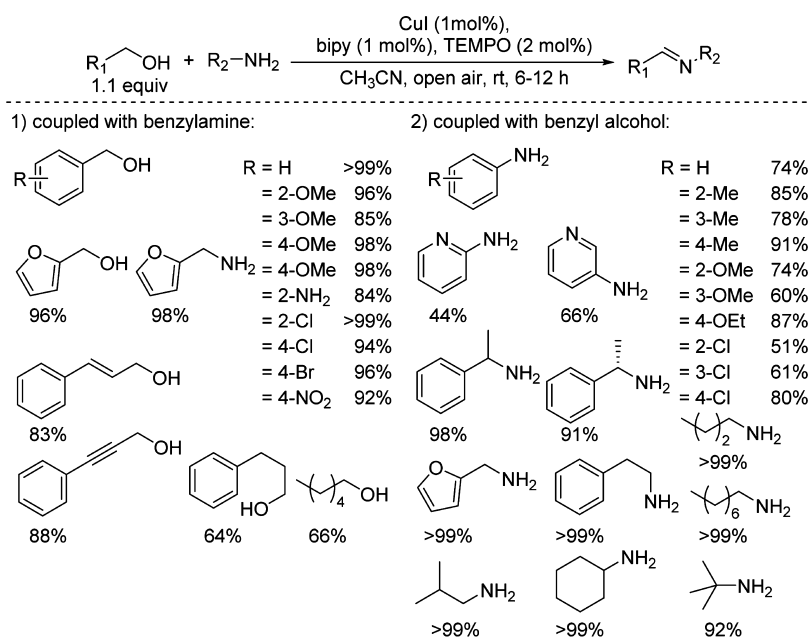
for the self-coupling of primary benzylic amines to produce homocoupled imines but also for the cross-coupling of benzylamines with electron-rich anilines to give the heterocoupled products. In addition, electron-rich anilines can undergo a self-coupling procedure to yield the corresponding azo compounds in the absence of benzylamines.

Similar reaction was also investigated by a  $\text{CuI}/\text{TEMPO}$  system under neat conditions. Secondary amines such as dibenzylamine and some cyclic amines can be selectively oxidized into the corresponding imine under relatively high temperatures

Scheme 5. CuBr/KetoABNO-Catalyzed Oxidation of Amines



Scheme 6. Cu/TEMPO-Catalyzed Cross-Coupling of Alcohols with Amines



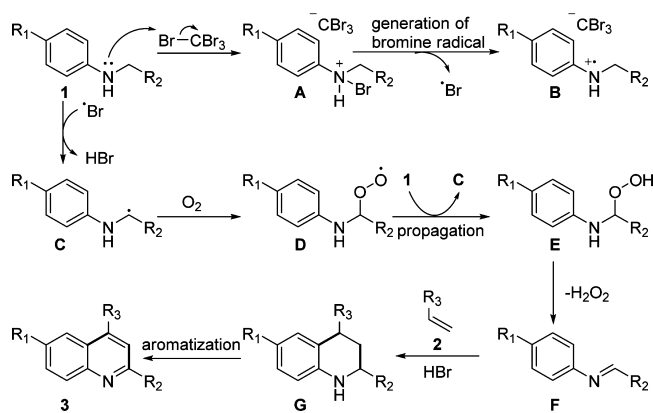
recycling experiments. Bai et al. also employed a lychee-shaped  $\text{Cu}_2\text{O}$  to accomplish the cross-coupling of benzylic alcohols with amines, whereas the issues of catalyst stability and additional base have still not been well solved.<sup>21</sup>

**Fe Catalysts.** Considering the fact that iron was an earth-abundant element and also compatible with nitroxyl derivatives, Xu et al. described a  $\text{Fe}(\text{NO}_3)_2/\text{TEMPO}$  system for both amine and alcohol oxidation with air as the oxidant.<sup>22</sup> Good to excellent yields were obtained for the self-coupling of primary amines, and high selectivity was achieved for the cross-coupling of benzylamine with some electron-rich anilines. Moreover, the cross-coupling of benzylic alcohols with aliphatic amines or anilines can also smoothly proceed after adding a catalytic amount of KOH. Thus, this catalytic system was practically useful as it provided several direct and greener approaches for the preparation of diverse imines.

As another iron-mediated reaction, the self-coupling of benzylamine was conducted in  $\text{CCl}_4$  solvent.<sup>23</sup> Interestingly, satisfactory results were only obtained with a large amount of

$\text{CCl}_4$ , and  $\text{CHCl}_3$  as well as HCl were detected after the reaction, revealing  $\text{CCl}_4$  was not only a solvent but also directly involved in the reaction. Consequently, it was proposed that  $\text{FeCl}_3$  catalyzed benzylamine and  $\text{CCl}_4$  to form *N*-chlorobenzylamine, followed by releasing HCl to give the key NH-imine intermediate. However, quite recently, Huo et al. showed that  $\text{CBr}_4$  can promote the oxidation of secondary amines and subsequent construction of quinoline derivatives without any additives.<sup>24</sup> The mechanism was depicted below (Scheme 7): the reaction of  $\text{CBr}_4$  with the substrate would first produce the intermediate **A**, which can undergo a homolytic cleavage of the weak N–Br bond to give the radical cation **B** and a bromine radical; after the C–H abstraction by the bromine radical, the amine substrate was transformed into the radical **C** and was promptly trapped by dioxygen to form the peroxide radical **D**, which can abstract a hydrogen atom from the substrate to give the hydroperoxide **E**; subsequent release of  $\text{H}_2\text{O}_2$  from **E** would give the desired imine **F**, and **F** can be further converted into quinoline derivatives via a Povarov reaction and the following aromatization. Control

### Scheme 7. CBr<sub>4</sub>-Catalyzed Oxidation of Secondary Amines to Construct Quinoline Derivatives



experiments confirmed that CBr<sub>4</sub>, rather than CHBr<sub>3</sub>, CH<sub>2</sub>Br<sub>2</sub>, and HBr, was the active species for this transformation.

Heterogeneous Fe-based metal–organic framework (Fe-MOF: Fe<sup>3+</sup> with 1,3,5-benzenetricarboxylate) incorporating *N*-hydroxyphthalimide (NHPI) was also investigated for amine oxidation.<sup>25</sup> Compared to supported noble catalysts, Fe-MOF/NHPI presented similar activity but better selectivity toward the self-coupling of benzylamine under solvent-free conditions. However, it failed to oxidize primary heterocyclic amines as well as secondary amines.

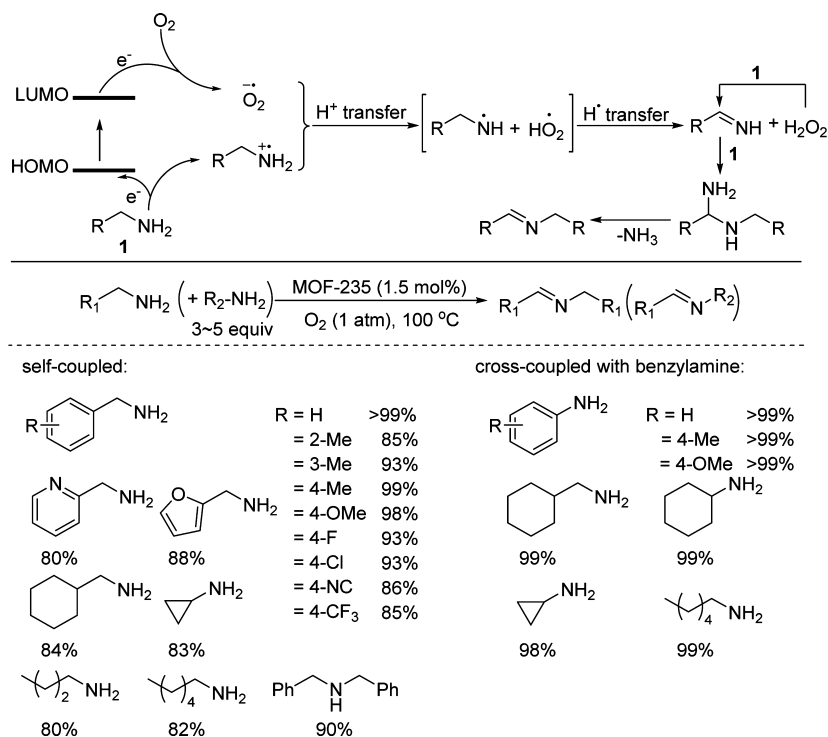
**Al Catalysts.** Li et al. recently reported an Al-based MOF (MOF-253: Al<sup>3+</sup> with 2,2'-bipyridine) for the coupling of primary amines under neat conditions.<sup>26</sup> Al<sup>3+</sup> in MOF-253 was not regarded as the active site on account of its full coordination, but 2,2'-bipyridine (bpy) moiety played a crucial role in activation of molecular oxygen, because the HOMO–LUMO gaps of bpy linker in MOF-253 were significantly decreased as

compared to the monomer, and the electrons were easily excited from the HOMO to the LUMO, which can reduce molecular oxygen to form superoxide radical anions (O<sub>2</sub><sup>•−</sup>). Thus, the amine substrates oxidized by the HOMO can further react with O<sub>2</sub><sup>•−</sup>, followed by H<sup>+</sup> and H· transfer processes to give NH-imine and H<sub>2</sub>O<sub>2</sub> intermediates. Meanwhile, the as-formed H<sub>2</sub>O<sub>2</sub> can also oxidize the substrates to produce NH-imines, which reacted with free amines and subsequently released NH<sub>3</sub> to produce the desired imines (Scheme 8). Notably, this catalytic protocol featured high activity and selectivity for both the homocoupled and heterocoupled imines, including some aliphatic products. What's more, MOF-253 can be reused at least six times without discernible loss in catalytic efficiency.

The activity of Al-grafted mesoporous silica (Al–MS) toward the amine oxidation at 160 °C was studied by the Mishra group.<sup>27</sup> It was demonstrated that the surface–OH groups of silanols played effective roles in amine activation via the formation of hydrogen bonds, and acid sites formed by incorporating appropriate amounts of Al could interact with the amino groups of amines to further improve the activity. This superiority, however, was only reflected in the self-coupling of primary benzylic amines. As for the cross-coupling of benzylamine with aniline, Al–MS showed slightly less activity than the simple MS, which might be attributed to the competitive adsorption of aniline over the strong acidic sites of Al–MS.

**V Catalysts.** In 2010, Ogawa et al. reported that oxygenated complex VO(Hhpic)<sub>2</sub> (H<sub>2</sub>hpic: 3-hydroxypicolinic acid) was active for the self-coupling of benzylamines at 120 °C and can be recovered using imidazolium-type ionic liquids as the solvent.<sup>28</sup> Subsequently, Gao et al. showed the reaction can be performed at 60 °C under air atmosphere by employing a more-active (HQ)<sub>2</sub>V<sup>v</sup>(O)(O<sup>i</sup>Pr) (HQ: 8-quinolinate).<sup>29</sup> Moreover, this catalyst showed moderate activity for the cross-coupling of alcohols with amines in the absence of any additives.

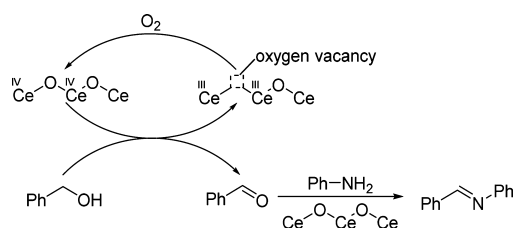
### Scheme 8. MOF-253-Catalyzed Imine Formation from Primary Amines



Heterogeneous vanadium compounds have also been explored for imine formation but underwent less-green and energy-efficient reactions, such as supported vanadium-substituted tungstophosphoric-acid-mediated self-coupling of primary amines under vapor-phase conditions,<sup>30</sup> whereas  $V_2O_5$  promoted the same reaction using  $H_2O_2$  as the terminal oxidant.<sup>31</sup>

**Ce Catalysts.** The redox properties of  $CeO_2$  in organic reactions at low temperature were first disclosed by the Tamura group, and they have been successfully applied in the synthesis of heterocoupled imines.<sup>32</sup> Kinetic experiments showed that the alcohol oxidation was the rate-determining step, and the condensation with amines can be promoted by the Lewis sites of  $CeO_2$ . Mass spectrum (MS) and Fourier transform infrared spectroscopy (FTIR) analysis demonstrated that the oxygen species at the redox sites of  $CeO_2$  were active for the oxidative dehydrogenation of alcohols, and the amount of these redox sites presented a good linearity with the reaction rate (Scheme 9).

**Scheme 9. Proposed Mechanism for the Cross-Coupling of Alcohols with Amines over  $CeO_2$**



Notably, the reaction can be conducted at 60 °C under air atmosphere, and excellent yields and selectivity were readily obtained for the coupling of benzyl alcohols with various anilines.

In an extension of this work, Wang et al. investigated the crystal-plane effects of  $CeO_2$  on the reaction.<sup>33</sup> The (110) plane was found to possess the strongest redox ability as it contained a higher concentration of oxygen vacancies than the other (100) and (111) planes. Besides, it was worth mentioning that the alcohol oxidation cannot proceed without amine substrates, implying the amines played a crucial role in removing the formed aldehydes to promote the whole reaction. Recycling experiments showed that the color of the catalyst was obviously changed, and remarkable deactivation was observed due to the poisoning of the active sites by the adsorption of organic species. Nevertheless, the activity can be recovered after calcination at 500 °C, and the reactivated  $CeO_2$  can be reused at least four times.

The self-coupling of primary amines with  $SiO_2$ -supported Sm-doped  $CeO_2$ <sup>34</sup> and Mo-doped  $CeO_2$ <sup>35</sup> at 120 °C under neat conditions have been recently studied by Reddy and co-workers. It was demonstrated that the dispersion of ceria-based oxides on  $SiO_2$  can improve  $CeO_2$  properties by reducing the particle size and increasing the surface area, and the introduction of Sm or Mo can facilitate the formation of oxygen vacancy defects in  $CeO_2$  and increase the acidic sites of the catalyst. For example, the conversion of benzylamine over  $CeO_2$ - $MoO_3$ / $SiO_2$  was up to

98%, but over  $CeO_2$ - $MoO_3$  and  $CeO_2$  were decreased to 65% and 16%, respectively. Applying these supported doped  $CeO_2$  in various substituted benzylamines oxidation, good to excellent yields were achieved. Moreover, the catalysts can be reused several times without the need of reactivation.

Similar reaction was also investigated by F-doped  $CeO_2$ .<sup>36</sup> The introduction of  $F^-$  was proposed to reduce the particle size, as well as increase the surface area and the concentration of  $Ce^{3+}/Ce^{4+}$  redox couple by reduction of  $Ce^{4+}$  to  $Ce^{3+}$ . With these benefits, F-doped  $CeO_2$  presented better efficiency than the undoped  $CeO_2$  toward the self-coupling of benzylamine derivatives under neat conditions.

**Mn Catalysts.** In 2008, Suib et al. reported that manganese octahedral molecular sieves (OMS-2) were active toward the cross-coupling of alcohols with amines under reflux conditions.<sup>37</sup> The average oxidation state of Mn was  $\sim 3.8$  containing  $Mn^{4+}$ ,  $Mn^{3+}$ , and  $Mn^{2+}$  ions in the framework. A Mars-van Krevelen type mechanism for the step of alcohol oxidation was proposed (Scheme 10): the slow oxidation of alcohols by  $Mn^{4+}$  would result in the formation of the carbocation intermediates and reduced  $Mn^{2+}$ ; then, the carbocations can be rapidly deprotonated into aldehydes, and further transformed into imine products in the presence of amines with the assistance of the Lewis sites of OMS-2; in the second half of the mechanism,  $O_2$  was adsorbed on the lattice vacancies of manganese oxides, and subsequently reduced by two electrons from the reduced  $Mn^{2+}$ ; because the formed lattice oxygen was easily released with the assistance of protons, these lattice vacancies can be recovered during the reaction.

Gao et al. subsequently utilized a supported manganese catalyst to fulfill the same reaction under milder conditions.<sup>38</sup> The activity was found to be strongly influenced by the surface properties of catalysts as the basic sites can promote the alcohol oxidation while the acidic sites were beneficial to the condensation step. Thus, amphoteric hydroxyapatite (HAP:  $Ca_{10}(PO_4)_6(OH)_2$ ) was selected as the best support, and the prepared  $MnO_x$ /HAP can efficiently catalyze the cross-coupling of various benzylic alcohols with an equimolar ratio of aromatic or aliphatic amines at 80 °C under air atmosphere (Scheme 11). Notably, both of the above two manganese-based catalysts showed good reusability after reactivation by calcinations.

Manganese oxides also showed potential activity toward amine oxidation.<sup>39</sup> After scanning various oxidative oxide catalysts, Wang et al. found the most active  $\alpha$ - $MnO_2$  can readily catalyze the self-coupling of primary benzylic and aliphatic amines at room temperature.<sup>40</sup> Nevertheless, *tert*-butyl hydroperoxide served as the terminal oxidant because considerable nitriles were formed using molecular oxygen as the oxidant.

Quite recently, Suib et al. disclosed that the same reaction can be realized employing air as the oxidant by a Cs ion-promoted mesoporous manganese oxide.<sup>41</sup> Surface  $Mn^{3+}$  species along with labile lattice oxygen were found to play important roles in promoting the catalytic activity, and the incorporation of trace amounts of Cs ions can enhance the basicity of the catalyst for the

**Scheme 10. Mechanism of Imine Synthesis Catalyzed by OMS-2**

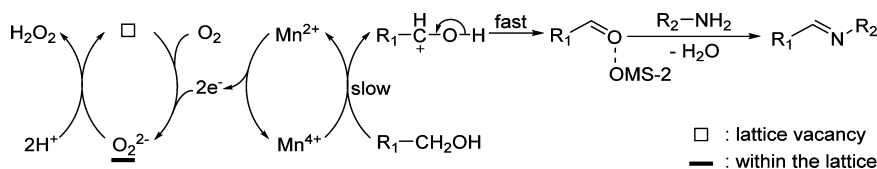




Table 1. Representative Data for the Oxidation of Primary and Secondary Amines over Gold-Based Catalysts

$$2 \text{Ph-CH}_2\text{-NH}_2 \left( \text{Ph-CH}_2\text{-N-CH}_2\text{-Ph} \right) \longrightarrow \text{Ph-CH=N-CH}_2\text{-Ph}$$

entry	catalyst	particle size (nm)	substrate <sup>a</sup>	temperature (°C)	P <sub>O<sub>2</sub></sub> (atm)	time (h)	TOF <sup>b</sup> (h <sup>-1</sup> )	ref
1	Au powder	~5 × 10 <sup>4</sup>	1°/2°	100	1	24	10 <sup>-3</sup> /10 <sup>-3</sup>	46, 47
2	Au/Al <sub>2</sub> O <sub>3</sub>	50–150	1°/2°	100	1	24	0.3/0.3	47
3	Au(OAc) <sub>3</sub>	10–50	2°	108	1	4	0.98	48
4	Au(OAc) <sub>3</sub> /CeO <sub>2</sub>	5–10	2°	108	1	8	7.2	48
5	Au(OAc) <sub>3</sub> +CeO <sub>2</sub>	5–10	1°/2°	108	1	16/5	3.2/9.3	49
6	Au(OAc) <sub>3</sub> +TiO <sub>2</sub>	–	2°	108	1	5	7.6	49
7	Au(OAc) <sub>3</sub> +SiO <sub>2</sub>	–	2°	108	1	5	7.8	49
8	Au(OAc) <sub>3</sub> +Al <sub>2</sub> O <sub>3</sub>	–	2°	108	1	5	9.4	49
9	HAuCl <sub>4</sub> ·3H <sub>2</sub> O+CeO <sub>2</sub>	–	2°	108	1	0.67	82	50
10	Au(OAc) <sub>3</sub> +FeO <sub>x</sub>	–	2°	108	1	5	8.4	51
11	Au(OAc) <sub>3</sub> +CeO <sub>2</sub> /FeO <sub>x</sub>	20	1°/2°	108	1	16/5	1.2/5.9	51
12	Au/TiO <sub>2</sub>	3.5	1°	100	5	30	3.3	52
13	Au/C	10	1°	100	5	1	99	52
14	PI–Au	~3	1°/2°	140/100	balloon	24	0.7/0.2	53
15	PI–Au	4–7	1°/2°	140/100	balloon	30/12	1.2/3.7	53
16	Au/CeO <sub>2</sub>	~5.3	1°	130	bubbling	4	2.4	54
17	Au/Ce <sub>0.9</sub> Fe <sub>0.1</sub> O <sub>2.8</sub>	~3.6	1°	130	bubbling	4	3.2	54
18	Au/CeO <sub>2</sub>	4–5	1°	100	3	6	64	56
19	Au/Graphite	14.5	2°	110	bubbling	17	1.2	57
20	Au/PMAS	9.6	2°	80	1	36	0.5	58b
21	Au/SBA-NH <sub>2</sub>	4–12	1°	100	1	24	4.9	59b
22	Au–Pd/Fiber	–	1°/2°	100	5	24	3.72/3.2	60
23	Au/Fiber	–	1°/2°	100	5	24	0.5/1.6	60

<sup>a</sup>Substrate: 1° (benzylamine); 2° (dibenzylamine). <sup>b</sup>TOF: (mol of substrate conversion)/(mol of gold × h).

alcohols into aldehydes. Pd–O<sub>2</sub> and Pd(II) species were crucial for the regeneration of TMEPO from the reduced TEMPOH, but they may also promote the alcohol oxidation with the assistance of base. Benzylic and aliphatic amines were effective coupling partners for various benzyl and cinnamyl alcohols, but for anilines derivatives, stoichiometric base must be introduced to increase their basicity and nucleophilicity.

Given additional additives and recycling problems of homogeneous palladium systems, Park et al. showed that palladium nanoparticles entrapped in boehmite nanofibers (Pd/AlO(OH)) can efficiently catalyze the coupling of substituted benzyl alcohols with a wide range of aromatic amines or aliphatic amines,<sup>43</sup> but aliphatic alcohols were sluggish and only gave an 8% yield. To overcome this drawback, Zhao et al. utilized Pd/ZrO<sub>2</sub> to fulfill the coupling of short-chain or branched aliphatic alcohols (C1–C6) with amines.<sup>44</sup> Despite the mild conditions (30 °C, air atmosphere), the presence of base KOH was critical for the reaction to proceed.

The oxidation of secondary amines over supported intermetallic Pd<sub>3</sub>Pb catalyst was studied by Komatsu and co-workers.<sup>45</sup> The proposed mechanism involved four steps: (1) adsorption of amine (N–H activation), (2) C–H activation, (3) desorption of the imine, and (4) removal of the hydrogen atom by O<sub>2</sub> (Scheme 13a). Among them, the first step was recognized as the rate-determining step and can be promoted by employing basic supports to facilitate the deprotonation of amines (Scheme 13b). Besides, the third step can be accelerated by introducing Pb atom because it has a considerably larger metallic radii than Pd (Pb: 1.75 Å; Pd: 1.37 Å), and thus the steric repulsion at Pd site was greater than that of monometallic Pd owing to the presence of the neighboring Pb atom. It was noteworthy that the desorption of imines would become the rate-determining step and the support effects would disappear for the supported

monometallic Pd catalyst, which further confirmed the indispensability of Pb atom. Excellent yields were achieved over Pd<sub>3</sub>Pb catalysts for various secondary aromatic, aliphatic, and cyclic amines, and high activity was also observed for the self-coupling of primary benzylic and aliphatic amines, but along with 8–21% nitrile byproducts.

**Au Catalysts.** *Au-Catalyzed Oxidation of Primary and Secondary Amines.* In 2007, Angelici et al. first reported the gold-catalyzed imine formation using molecular oxygen as the terminal oxidant.<sup>46</sup> Bulk gold powder (50 μm) was found to be quite capable of oxidizing various secondary amines and benzylamine under relatively mild conditions (Table 1, entry 1), but low productivity (TOF: ~ 10<sup>-3</sup> h<sup>-1</sup>) was observed as most gold atoms in bulk have not been utilized. Subsequently, they employed Au/Al<sub>2</sub>O<sub>3</sub> (50–150 nm) to fulfill the same reaction, and the yields as well as TOFs were significantly increased (Table 1, entry 2).<sup>47</sup> In line with these results, the performance of nanogold was studied by the Baiker group. By simply adding Au(OAc)<sub>3</sub> or Au(OAc)<sub>3</sub> preadsorbed on CeO<sub>2</sub> into the reaction, gold nanoparticles (10–50 nm) or supported gold nanoparticles (5–10 nm) can be formed in situ and were very active in amine oxidation.<sup>48</sup> The TOF of the former was 980 times higher than that of bulk gold powder, and the later was 22 times higher than that of Au/Al<sub>2</sub>O<sub>3</sub> for the oxidative dehydrogenation of dibenzylamine (Table 1, entries 3–4), suggesting the efficiency of gold catalysts was strongly influenced by gold size as well as the supports.

In 2009, Baiker et al. revealed that the preparation of supported gold catalysts can be further simplified by directly adding Au(OAc)<sub>3</sub> and CeO<sub>2</sub> into the reaction without the need of preadsorption process, and other common supports such as TiO<sub>2</sub>, SiO<sub>2</sub> and Al<sub>2</sub>O<sub>3</sub> were also suitable for this in situ preparation method (Table 1, entries 5–8).<sup>49</sup> Besides, they



found the  $\text{Au}(\text{OAc})_3/\text{TiO}_2$  with larger gold size and uneven particle dispersion was more active than the commercial  $\text{Au}/\text{TiO}_2$ , and the catalytic efficiency for indoline oxidation was much higher than dibenzylamine oxidation because the gold size in the presence of the former was remarkably smaller than in the latter. Thus, these results implied that the particle size was a key but not the only factor affecting the performance of gold catalysts, and the formation of these nanoparticles was influenced by the amine substrates using this in situ preparation method, which can in turn affect the amine own oxidation.

In the subsequent work, they investigated the anions of gold precursors on amine oxidation, and found chlorine-containing gold salt was the best precursor to prepare supported gold catalysts. The TOF of  $\text{HAuCl}_4 \cdot 3\text{H}_2\text{O} + \text{CeO}_2$  for dibenzylamine oxidation was up to  $82 \text{ h}^{-1}$  (Table 1, entry 9).<sup>50</sup> Besides, they also studied the catalyst recyclability by employing a superparamagnetic  $\text{CeO}_2/\text{FeO}_x$  as the support since the obtained catalyst can be easily separated by magnet.<sup>51</sup> Although the activity was somewhat lower than using either  $\text{FeO}_x$  or  $\text{CeO}_2$  as the support (Table 1, entries 5, 10–11), the deactivation of  $\text{Au}(\text{OAc})_3 + \text{CeO}_2/\text{FeO}_x$  can be greatly suppressed. In addition, the loss of activity of the catalyst prepared by adsorption method ( $\text{Au}(\text{OAc})_3/\text{CeO}_2$ ) was only half as the catalyst by direct addition ( $\text{Au}(\text{OAc})_3 + \text{CeO}_2$ ) in reuse tests. The above results indicated the stability of gold catalysts was greatly influenced by the properties of the supports and the catalyst preparations. On the other hand, the leaching and sintering of active species were also often encountered in heterogeneous catalysis. A rapid decrease of conversion (21%) was still observed over  $\text{Au}/\text{Al}_2\text{O}_3$  prepared after heating at  $700 \text{ }^\circ\text{C}$  for 68 h, clearly demonstrating the sintering of gold nanoparticles was not the key factor in this catalytic system.

The relationship between the activity and gold crystallite size was systematically investigated by Corma, Garcia, and co-workers.<sup>52</sup> An exponential increase of activity was observed as the gold particles of  $\text{Au}/\text{TiO}_2$  decreased from 25 to 3.5 nm, implying the reaction was structure sensitive, and the active unsaturated gold atoms located at the corners of the crystallites increased with the decrease of gold crystal size. However, in an attempt to achieve a higher metal dispersion by employing high surface area support, they found commercial  $\text{Au}/\text{C}$  containing 10 nm gold particle was 30 times more active than the best  $\text{Au}/\text{TiO}_2$  (Table 1, entries 12–13), which further confirmed that the activity of gold was not only influenced by the particle size but also by the supports.

Kobayashi et al. also studied the size effect of gold-cluster on amine oxidation.<sup>53</sup> Polymer-incarcerated Au nanoclusters (PI–Au) with relatively larger clusters (>5 nm) were found to be more active than the catalyst containing smaller clusters (3 nm) at  $100 \text{ }^\circ\text{C}$  (Table 1, entries 14–15). In addition, the catalyst with high gold loading showed better catalytic activity than that with low loading at  $100 \text{ }^\circ\text{C}$ , and both of the catalysts presented higher activity in reuse tests than fresh experiment. Transmission electron microscopy (TEM) analysis showed that the average cluster size of the recycled catalyst with high loading increased from 3.8 to 16.0 nm, and with low loading, the cluster size increased from 3.0 to 6.9 nm, revealing small Au clusters less tightened to polymer were easily aggregated during the reaction, particularly with a high loading. Besides, high reaction temperature can also promote the particle aggregation by swelling the polymer because both of the fresh catalysts gave similar yields at  $140 \text{ }^\circ\text{C}$ . All these results disclosed that the catalytic efficiency was not always increased by continuously reducing the gold particles,

and the optimized size may depend on the balance of adsorption of substrate and product since the relative adsorption strength of imine against amine on small gold clusters was larger than on large clusters. Utilizing a polymer containing tertiary amine groups as the support was an effective approach to eliminate the adsorbed imine because of their nucleophilicity and bulkiness and thus could make the catalytic cycle faster.

Nanocrystalline  $\text{Fe}_{0.9}\text{Ce}_{0.1}\text{O}_{1-\delta}$  supported gold catalyst for the self-coupling of benzylamine has been recently explored by the Reddy group.<sup>54</sup> It was revealed that the synergetic effects between Au and the support can be improved by doping appropriate iron, and the obtained  $\text{Au}/\text{Fe}_{0.9}\text{Ce}_{0.1}\text{O}_{1-\delta}$  with smaller gold nanoparticles presented better activity than  $\text{Au}/\text{CeO}_2$  (Table 1, entries 16–17). In addition, they found the catalytic efficiency was highly dependent on the preparation method as the catalyst prepared by deposition–precipitation was more active than by anionic exchange. Porous silica containing Ce–Ni mixed oxides supported gold catalysts were studied by the Parvulescu group.<sup>55</sup> Curiously, the supports themselves showed considerable activity for the benzylamine oxidation at  $75 \text{ }^\circ\text{C}$ , and significant enhancement by gold was observed until the temperature increased to  $115 \text{ }^\circ\text{C}$ . Gold size and the components of the support including the ratio of Ce/Ni were proposed to greatly affect the final performance of the catalysts.

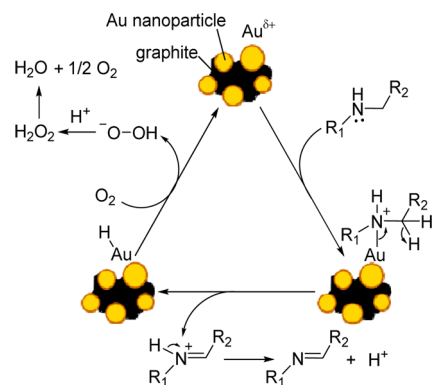
Apart from doping a secondary element, Wang et al. reported that the crystal plane of ceria was also crucial for the performance of  $\text{Au}/\text{CeO}_2$ .<sup>56</sup> Oxygen vacancy sites were proposed to be easily formed at the crystal planes of (110), and were beneficial for the absorption of gold to construct a strong gold–ceria interaction. X-ray photoelectron spectroscopy (XPS) showed that 71% gold were positively charged in  $\text{Au}/\text{CeO}_2$ , which can greatly lower the C–H bond activation energy of amine substrates. The TOF of benzylamine oxidation was up to  $64 \text{ h}^{-1}$  and was much higher than that reported  $\text{Au}/\text{CeO}_2$  (Table 1, entry 18).

Graphite-supported gold nanoparticles were investigated by the Che group, and good yields were achieved with various secondary and electron-rich primary benzylic amines.<sup>57</sup> Although the TOF was not outstanding (Table 1, entry 19),  $\text{Au}/\text{graphite}$  can be reused for 10 consecutive runs without apparent deterioration. Kinetic experiments showed that the C–H bond cleavage at the benzylic position was the rate-determining step; positively charged intermediates were generated during the reaction, and oxygen pressure has no significant effect on the initial reaction rate. On the basis of these results, amines were proposed to coordinate on the surface  $\text{Au}^{\delta+}$  sites, followed by C–H bond cleavage to give the desired imines. Then, the hydrogen on the surface of gold was removed by dioxygen (Scheme 14).

Gold nanoparticles supported on poly(2-methoxyaniline-5-sulfonic acid) (PMSA)<sup>58</sup> or amine-functionalized mesoporous silica (SBA-15- $\text{NH}_2$ )<sup>59</sup> have also been investigated for amine oxidation (Table 1, entries 20–21). The supports played multiple roles: for PMSA, it not only served as a stabilizer for Au particles but also as a redox mediator for the transference of hydrogen leaving from amines; for SBA-15- $\text{NH}_2$ , the functionalized amine nitrogen could stabilize Au particles, and the  $\pi$  electrons of vinyl groups on SBA-15 can interact with the d-band of Au.

The combination of gold and palladium was explored by the Repo group.<sup>60</sup> Au–Pd alloy deposited on porous steel fiber matrix ( $\text{Au–Pd}/\text{fiber}$ ) via a sputtering technique was more active than  $\text{Au}/\text{fiber}$  and  $\text{Pd}/\text{fiber}$  for both primary and secondary amines oxidation (Table 1, entries 22–23). It was demonstrated that Pd atoms not only assisted the cleavage of C–H and N–H

### Scheme 14. Proposed Mechanism of Au/C-Catalyzed Imine Formation



bonds of amines but also served as a diluent to improve Au dispersion to form smaller Au nanoparticles.

**Au-Catalyzed Cross-Coupling of Alcohols with Amines.** In 2009, Cao et al. first reported the cross-coupling of alcohols and amines by supported gold catalysts.<sup>61</sup> Compared to other supports (C, CeO<sub>2</sub>, Fe<sub>2</sub>O<sub>3</sub>, TiO<sub>2</sub> and β-Ga<sub>2</sub>O<sub>3</sub>), hydroxyapatite (HAP: Ca<sub>10</sub>(PO<sub>4</sub>)<sub>6</sub>(OH)<sub>2</sub>), which possesses unique amphoteric character, was found to be the best support as the surface basicity of Au/HAP can promote alcohol oxidation, and the acid sites can significantly accelerate the condensation of aldehydes with amines (Table 2, entries 1–5). Other catalysts such as Pd/HAP and Ru/HAP were also investigated but presented poor activity, implying gold was far superior to other noble metals for this coupling reaction. Various primary benzylic, allylic, and even aliphatic alcohols can effectively react with anilines or aliphatic amines (Scheme 15). Moreover, this system can be applied to the one-pot synthesis of α-aminophosphonates and oximes.

Following this work, Hensen et al. investigated the performance of hydrotalcite (HT: Mg<sub>1-x</sub>Al<sub>x</sub>(OH)<sub>2</sub>(CO<sub>3</sub>)<sub>x/2</sub>·nH<sub>2</sub>O) supported gold catalysts (Table 2, entry 6).<sup>62</sup> The activity was found to be strongly influenced by the Mg/Al ratio, and after the ratio was adjusted from 2 to 6, both the initial alcohol oxidation and the subsequent condensation were hindered due to the decrease of surface area and increasing basicity, respectively. Cationic gold species were supposed to act as Lewis acid sites to facilitate the condensation step; however, this effect was not obvious as the amine substrates were mainly limited to strong

nucleophilic aliphatic amines, and considerable aldehydes were still observed in some cases.

Au/TiO<sub>2</sub><sup>63</sup> and Au/ZrO<sub>2</sub><sup>64</sup> have also been explored for this cross-coupling reaction, but additional KOCH<sub>3</sub> was crucial for the reaction to start as it could promote the deprotonation of alcohols to form metal-alkoxides and facilitate the aldehyde formation (Table 2, entries 7–8). To solve this issue, bimetallic Au–Pd/ZrO<sub>2</sub> was introduced, and excellent yields were achieved for alcohol oxidation in the absence of any additives.<sup>65</sup> However, due to the competitive adsorption on the active sites, the catalyst became completely inactive upon adding amines. Consequently, amines were added until alcohols were completely consumed, and the subsequent condensation were efficiently performed within 1 h (Table 2, entry 9).

Kobayashi et al. showed that the polymer-incarcerated carbon black (PICB) supported Au–Pd nanoparticles can accomplish the same reaction by simultaneously adding alcohols and amines (Table 2, entry 10).<sup>66</sup> The Pd atoms in the Au–Pd alloy, being more electropositive and expressing strong Lewis acid character, can accelerate the condensation step to achieve high selectivity. Meanwhile, the solvent 2,2,2-trifluoroethanol (TFF), with Brønsted acid and/or hydrogen-bond donor properties, can also promote this procedure. Primary benzylic, propargyl, allylic, and aliphatic alcohols can be efficiently coupled with various aromatic or aliphatic amines. Furthermore, the catalyst presented excellent recyclability.

Similar work was also reported by the Zhang group (Table 2, entry 11).<sup>67</sup> Interestingly, the reaction pathways can be switched by the ratio of Au/Pd: amides were produced on Au<sub>6</sub>Pd/resin, and imines were obtained over AuPd<sub>4</sub>/resin. These results can be rationalized by the differences of adsorption strength of aldehyde intermediates on the catalyst surface: in the case of Au<sub>6</sub>Pd/resin, adsorbed aldehyde species tended to form because of the strong affinity of Au, and subsequently, they reacted with amines to form adsorbed hemiaminals, followed by further oxidation to give amides; as for AuPd<sub>4</sub>/resin, free aldehydes were preferentially formed owing to the isolation of Au atoms by Pd which weakened the adsorption of aldehydes on Au atoms. So, upon formation, the free aldehydes were coupled with amines to produce imines. In both above Au/Pd systems, additional NaOH was introduced to promote the reaction because the polymers themselves did not contain any basic sites.

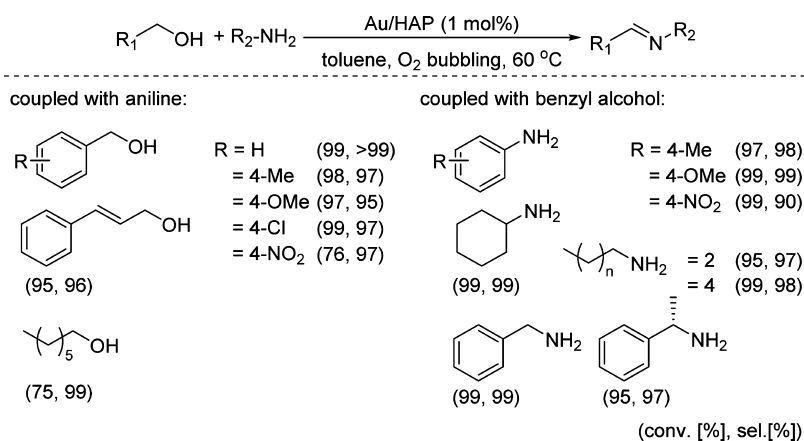
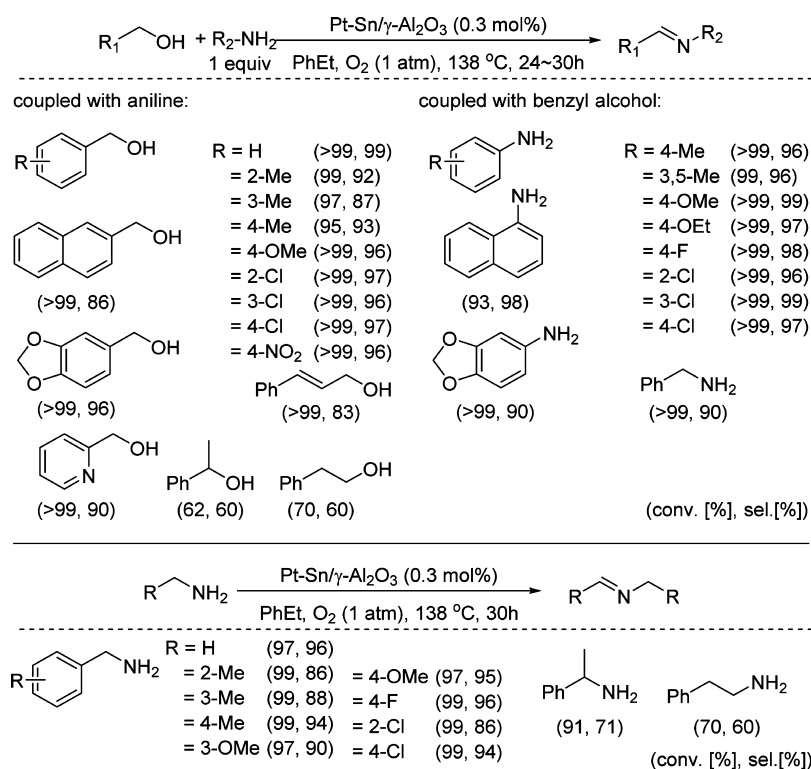
**Ag Catalysts.** Kegnæs et al. showed that Ag/Al<sub>2</sub>O<sub>3</sub> exhibited high selectivity for the cross-coupling of primary benzylic

Table 2. Representative Data for the Cross-Coupling of Alcohols and Amines over Gold-Based Catalysts

		Ph-CH <sub>2</sub> -OH + Ph-NH <sub>2</sub> → Ph-CH=N-Ph							
entry	catalyst	particle size (nm)	substrate ratio <sup>a</sup>	temperature (°C)	P <sub>O<sub>2</sub></sub> (atm)	time (h)	TOF (h <sup>-1</sup> ) <sup>b</sup>	ref	
1	Au/HAP	3.6 nm	1:1	60	bubbling	3	33	61	
2	Au/CeO <sub>2</sub>	–	1:1	60	bubbling	3	17.6	61	
3	Au/Fe <sub>2</sub> O <sub>3</sub>	–	1:1	60	bubbling	3	3.3	61	
4	Au/TiO <sub>2</sub>	–	1:1	60	bubbling	3	12	61	
5	Au/β-Ga <sub>2</sub> O <sub>3</sub>	–	1:1	60	bubbling	3	4.3	61	
6	Au/Mg <sub>2</sub> Al-HT	2.1 nm	1:1	60	bubbling	3	– <sup>c</sup>	62	
7	Au/TiO <sub>2</sub>	4–8 nm	1:1	20	1	24	14.5	63	
8	Au/ZrO <sub>2</sub>	2–7 nm	1:0.5	60	1	24	0.8	64	
9	Au–Pd/ZrO <sub>2</sub> (two steps)	4.6 nm	1:1	40	1 (air)	7 + 1	35.3 <sup>d</sup>	65	
10	PICB-Au/Pd	–	1:1	60	balloon	12	3.9 <sup>d</sup>	66	
11	Au–Pd/resin	2.3 nm	1.5:1	40	balloon	12	2.2 <sup>d</sup>	67	

<sup>a</sup>Substrate ratio: (mol of benzyl alcohol)/(mol of aniline). <sup>b</sup>TOF: (mol of substrate conversion)/(mol of Au × h). <sup>c</sup>Not calculated. <sup>d</sup>Based on the total moles of Au and Pd.

Scheme 15. Tandem Synthesis of Imines from Various Alcohols and Amines Using Au/HAP

Scheme 16. Direct Synthesis of Imines over Pt-Sn/ $\gamma$ -Al<sub>2</sub>O<sub>3</sub>

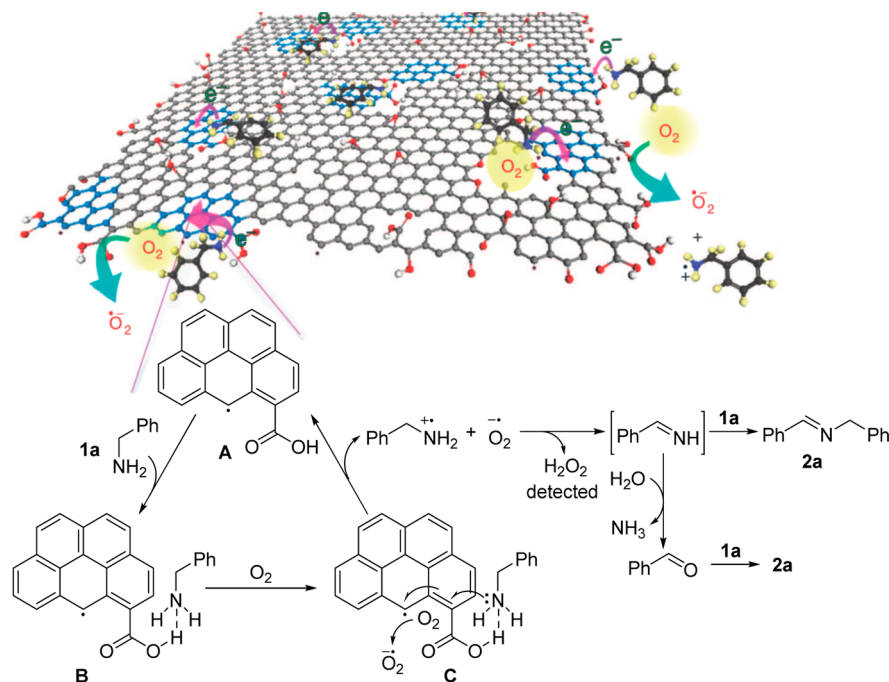
alcohols with anilines or aliphatic amines.<sup>68</sup> Interestingly, performing the reaction under air atmosphere would give better performance than under pure O<sub>2</sub>, suggesting a small amount of oxygen was efficient to remove the hydrogen on the Ag atoms, and high partial pressure of O<sub>2</sub> may oxidize the active Ag into inactive Ag<sub>2</sub>O. The same reaction was also examined by Ag-NHC (NHC: N-heterocyclic carbene) complexes with stoichiometric base.<sup>69</sup> Benzyl and allylic alcohols can be smoothly coupled with various aromatic or aliphatic amines under room temperature. Besides, alcohols can be selectively oxidized into aldehydes or carboxylic acids by changing the type of base and the reaction temperature.

**Ir Catalysts.** The amine oxidation by iridium oxide nanoparticles (Ir/CeO<sub>2</sub>) was investigated by the Hermans group.<sup>70</sup> A Langmuir–Hinshelwood relationship between the initial rate and the substrate concentration was presented, and the concentration corresponding to the maximum achievable

rate ( $V_{\max}$ ) for the self-coupling of benzylamine was significantly lower than that required for the oxidation of benzyl alcohol, implying the equilibrium between the adsorbed and free substrates was more readily achieved with amines. Besides, it was found that the selectivity was influenced by the ratio of amine/catalyst: at high free amine concentrations, NH-imine intermediate was displaced and can undergo hydrolysis/condensation to give the desired imine; however, at low concentrations, the intermediate was consecutively dehydrogenated into benzonitrile byproduct on available catalyst surface. This phenomenon was also observed in Ru-based and Au-based catalytic systems, because the former was often performed at lower amine/catalyst ratios (20–40) to produce nitriles, and the latter was conducted at higher ratios (>100) but to give imine products.

**Ru Catalysts.** Homogeneous Ru-based complexes were greatly explored for amine oxidation, but the reactions were

Scheme 17. Mechanism of GO-Catalyzed Self-Coupling of Primary Amines



conducted under inert atmospheres and harsh conditions.<sup>6d–j</sup> However, supported Ru catalysts often promoted nitrile formation from benzylamines.<sup>4a</sup> Nevertheless, in 2009, Mizuno et al. showed that Ru(OH)<sub>x</sub>/TiO<sub>2</sub> can efficiently catalyze the cross-coupling of primary benzylic or cinnamyl alcohols with anilines or aliphatic amines.<sup>71</sup> Ru/HAP, consistent with results of Cao,<sup>61</sup> was inactive, and RuCl<sub>x</sub>/TiO<sub>2</sub> as well as various Ru complexes all failed to promote the reaction, suggesting ruthenium hydroxide species on supports was important to achieve high catalytic performance. Following this work, Ramón et al. revealed that Ru(OH)<sub>3</sub>/Fe<sub>3</sub>O<sub>4</sub> can fulfill the same reaction under inert atmosphere, and the additional base can switch the final products: imines were obtained with NaOH, while alkylated anilines were formed in the presence of KOH.<sup>72</sup>

**Pt/Sn Catalysts.** In 2011, Yu et al. found the bimetallic Pt–Sn/ $\gamma$ -Al<sub>2</sub>O<sub>3</sub> (Pt/Sn = 1:3) can promote both alcohol and amine oxidation to the synthesis of imines at relatively high temperatures and long reaction times.<sup>73</sup> It was proposed that alcohol or amine substrates were initially dehydrogenated into aldehyde or NH-imine intermediates with the concomitant formation of [PtSn] hydrides. Then, the target imines were formed by the condensation of the intermediates with free amines. Notably, the hydrogen of metal hydrides can be either removed by oxygen under aerobic conditions or can be accepted by the as-formed imine products to further synthesize secondary amines under inert atmosphere. The doped Sn was regarded as a spacer to disperse Pt particles and improve electronic properties of Pt atoms, and the  $\gamma$ -Al<sub>2</sub>O<sub>3</sub> with Lewis sites can facilitate the condensation steps. Excellent yields were achieved for both the cross-coupling of benzyl alcohols with anilines and the self-coupling of primary benzylic amines (Scheme 16). Moreover, some secondary and aliphatic alcohols as well as amines were also suitable for this system, and the catalyst showed good recyclability.

**Base Catalysts.** In 2012, Tang et al. employed stoichiometric KOH to accomplish the cross-coupling of benzyl alcohols with anilines or aliphatic amines at 90 °C under air atmosphere.<sup>74</sup>

Alkoxide intermediates were proposed to be generated from alcohols with the assistance of base, which were further transformed into aldehydes, followed by the condensation with amines to produce the target imines. Because no desired product was detected under nitrogen atmosphere, molecular oxygen may have also played a significant role in the catalytic reaction. A similar reaction was examined by Adimurthy et al. using 10 mol % NaOH under neat conditions.<sup>75</sup> Besides base and O<sub>2</sub>, the amine substrates were found to be necessary for the activation of alcohols to produce the aldehyde intermediates.

### 3. METAL-FREE CATALYSTS

Given the wide applications of imine derivatives in pharmaceutical and biotechnological industries, it was highly desirable to perform the reaction under metal-free conditions to avoid metal contamination.

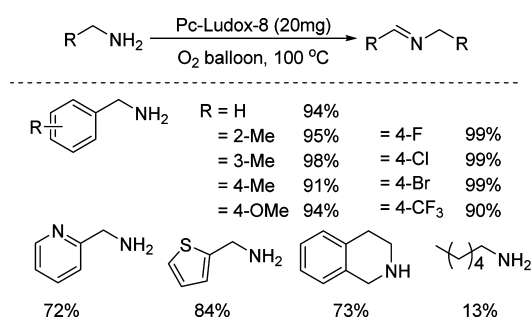
**Heterogeneous Metal-Free Systems.** In 2012, the groups of Cao<sup>76</sup> and Loh<sup>77</sup> independently reported the graphene oxide (GO)-mediated imine formation from primary amines. In the Cao report, both high catalyst loading (50 wt %) and oxygen pressure (5 atm) were required. By monitoring the reaction, a notable amount of aldehyde was observed at the initial stage, and the introduction of H<sub>2</sub>O can greatly accelerate the reaction. Thus, aldehyde generated from the hydrolysis of NH-imine was proposed as the key intermediate. Meanwhile, Loh et al. found the activity of GO was significantly influenced by the post-treatments. For instance, performing the self-coupling of benzylamine with oxygen in CH<sub>3</sub>CN at 80 °C for 5 h, GO only gave the corresponding imine in 44% yield, while the GO after base treatment and acid reprotonation would produce the product in 89% yield. In addition, the catalytic activity can be remarkably enhanced by increasing the concentration of the substrates. Therefore, various primary benzylic amines can be readily self-coupled with 5 wt % GO under neat conditions. Catalyst characterization combined with control experiments revealed that the carboxylic acid groups and unpaired electrons at the edge defects of GO constituted the active sites, which trapped

both molecular oxygen and amine substrates to promote the subsequent transformations (Scheme 17).

B, N-codoped holey graphene (BNG) was also active for amine oxidation.<sup>78</sup> The HOMO–LUMO gaps were proposed to be reduced by doping boron atoms to lower the HOMO levels and by doping nitrogen atoms to elevate the LUMO levels. Consequently, the active sites can easily induce electron relocation to activate both amine substrates and molecular oxygen. In addition, the catalytic efficiency can be further enhanced by the combination of BNG with carbon nanotubes as the formation of multiple nanoscale carbon p–n junctions were beneficial to the activation of molecular oxygen.<sup>79</sup>

Mesoporous carbons derived from macrocyclic compounds such as phthalocyanine (Pc) and porphyrin also presented good performance for the self-coupling of primary benzylic amines (Scheme 18).<sup>80</sup> For example, the self-coupling of benzylamine at

**Scheme 18. Self-Coupling of Primary Amines over Pc-Ludox-8**

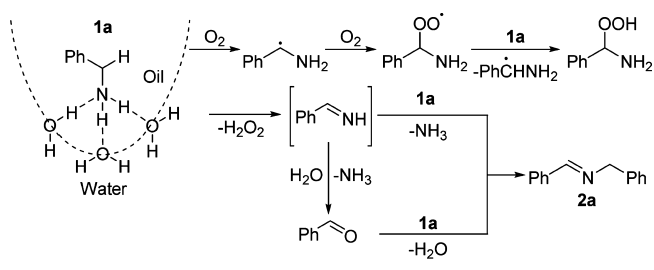


a 100 mmol scale can smoothly proceed with only 0.47 wt % mesoporous carbon under neat conditions, and the catalyst can be reused at this scale for several times without the need of additional reactivation treatment, which highlighted the practical application of these materials. Defect sites generated from the pyrolysis procedure as well as surface area and pore volume were proposed as the crucial factors for the carbon catalysts to achieve high activity.

**Homogeneous Metal-Free Systems.** In 2011, Fu et al. revealed that the coupling of primary amines can be realized by refluxing the suspensions of substrates and water under 1 atm dioxygen without any additives.<sup>81</sup> The amount of water was found to be crucial for the reaction, and the highest yield was achieved when the volume ratio of water to amine was 8 to form a biphasic system. Various primary benzylic amines can be smoothly self-coupled to give the homocoupled imines in 51–89% yields, and also, they can be cross-coupled with anilines or aliphatic amines to produce the heterocoupled imines in 45–77% yields. The reaction mechanism was proposed as follows: on the phase interface, benzylamine was first activated by forming hydrogen bonds with water; then, dioxygen grabbed the  $\alpha$ -H of benzylamine to form the benzyl radical, which reacted with oxygen to further form the peroxide complex; after releasing H<sub>2</sub>O<sub>2</sub>, the complex was transformed into NH-imine intermediate, followed by direct attack or hydrolysis/condensation processes to give the target imine (Scheme 19).

Ionic liquids (IL), for instance, tetra-butylammonium bromide (TBABr), also showed high efficiency toward amine oxidation.<sup>82</sup> Because the formation of hydrogen bond was determined by the capability of IL anion, AcO<sup>−</sup>, Cl<sup>−</sup>, and Br<sup>−</sup> promoted the reaction much better than BF<sub>4</sub><sup>−</sup> and PF<sub>6</sub><sup>−</sup>. Meanwhile, the water in the IL has a detrimental effect in terms of the competitive hydrogen

**Scheme 19. Possible Mechanism for the Cross-Coupling of Amines in a Biphasic System**



bond with substrates. The reaction was proposed to start with a direct single-electron transfer from benzylamine to dioxygen, which resulted in the formation of the radical ion pair ( $1a^{+\bullet} O_2^{-\bullet}$ ). Notably, this ion pair can be particularly stabilized by solvation in IL, as a result of ion–ion interactions with the ionic components of the solvent, and also by hydrogen bonds between the radical  $1a^{+\bullet}$  and the IL anions. Subsequent dehydrogenation of  $1a^{+\bullet}$  by  $O_2^{-\bullet}$  would give rise to the NH-imine intermediate, which further condensed with the starting substrate to give the desired imine. Given the absence of aldehyde during the reaction, other pathways might be unfavorable to this system (Scheme 20). Hammett plots revealed that the rate-determining step for electron-deficient benzylamines was the formation of the ion pair, but for electron-rich benzylamines, the rate-determining step was the dehydrogenation process. Benzylamine derivatives and dibenzylamine were readily transformed into the homocoupled imines in 88–99% yields, and some relatively inert amines like diphenyl- and cyclohexyl- methanamines also presented good results. Moreover, the cross-coupling of benzylamine with different amines can be effectively carried out, and excellent selectivity was observed when aliphatic amines served as the partners.

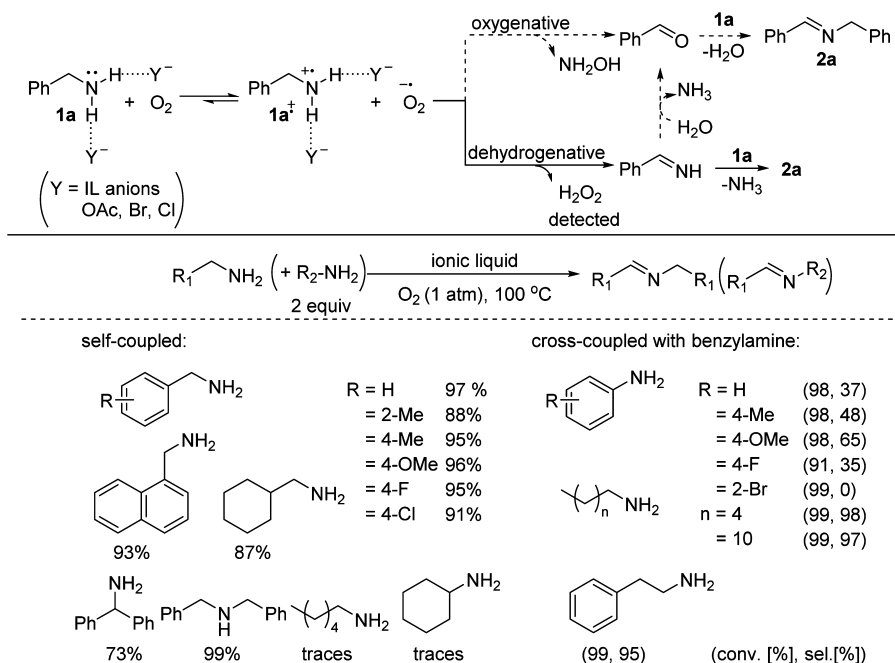
The utilization of azobis(isobutyronitrile) (AIBN) as a radical initiator for imine formation was explored by the Fu group, and various primary benzylic amines can be transformed into the homocoupled imines in 46–89% yields. In addition, the cyanation of tertiary amines to prepare  $\alpha$ -aminonitriles were also suitable for this catalytic system.<sup>83</sup> The mechanism was depicted in Scheme 21: in the initiation stage, AIBN was first decomposed into 2-cyano-2-propyl radical (CP<sup>•</sup>), followed by the combination with O<sub>2</sub> to form the alkylperoxyl radical CPOO<sup>•</sup>; subsequent release of one molecule of O<sub>2</sub> from two CPOO<sup>•</sup> would lead to two alkyloxyl CPO<sup>•</sup>; then, the active CPO<sup>•</sup> grabbed a hydrogen atom from benzylamine to form the  $\alpha$ -aminoalkyl radical A, which was readily trapped by O<sub>2</sub> to generate the peroxide radical B; similar to CPO<sup>•</sup>, B can capture a hydrogen atom from the substrate to produce the hydroperoxide C; after releasing H<sub>2</sub>O<sub>2</sub>, C was converted into the NH-imine intermediate and finally condensed with free benzylamine to give the target imine.

#### 4. PHOTOCATALYSTS

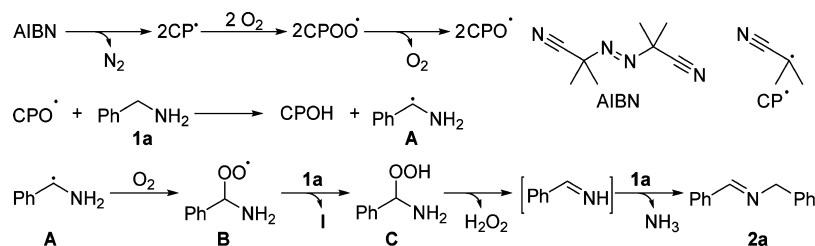
Recently, the utilization of sunlight as an energy force for chemical reactions has attracted intensive attention and has also brought along the great development of photocatalysts for imine formation.<sup>84</sup>

**Heterogeneous Photocatalytic Systems.** In 2011, Zhao et al. first disclosed TiO<sub>2</sub> (Degussa P125)-mediated imine formation from amines under ultraviolet-light irradiation.<sup>85</sup> Subsequently, they found the surface complex formed by

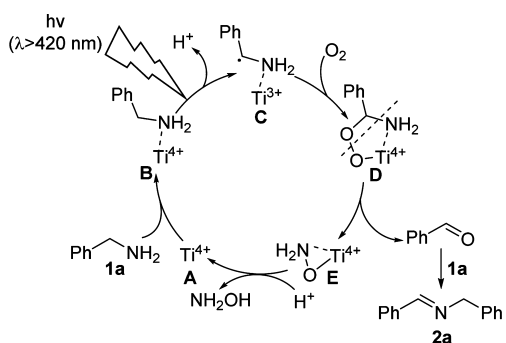
## Scheme 20. Ionic-Liquid-Mediated Imine Formation from Primary Amines



## Scheme 21. Proposed Mechanism of AIBN-Initiated Amine Oxidation



adsorption of amine on  $\text{TiO}_2$  can serve as an antenna to absorb visible light and thus successfully extend the reaction to the visible-light region.<sup>86</sup> The proposed mechanism was displayed in Scheme 22: the antenna B, excited by visible light, would first

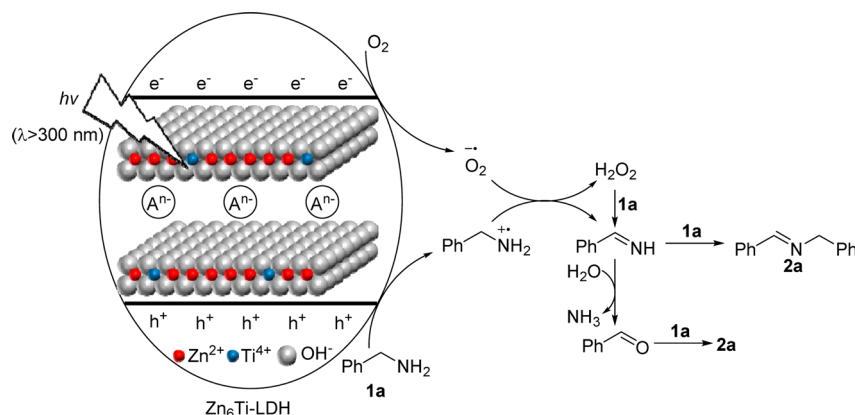
Scheme 22. Proposed Mechanism of Amine Oxidation Catalyzed by  $\text{TiO}_2$ 

generate the hole–electron pairs; then, the holes localized on the adsorbed amine promoted the deprotonation of amine to form the neutral carbon-centered radical C; meanwhile, the electrons localized within the  $\text{TiO}_2$  lattice resulted in the formation of  $\text{Ti}^{3+}$  ions; both C and  $\text{Ti}^{3+}$  were easily combined with  $\text{O}_2$  to produce the oxygen bridge intermediate D, which underwent a cleavage of C–N bond and O–O bond to release aldehyde intermediate,

followed by the condensation with free amine to give the desired imine; finally,  $\text{TiO}_2$  was recovered from the complex E with the assistance of  $\text{H}^+$ . Good to excellent yields were obtained for the self-coupling of various benzylic amines. However, a mixture of aldehydes, symmetric and unsymmetric imines was observed for the oxidation of substituted dibenzylamines, suggesting a similar pathway like the primary amine oxidation rather than a direct oxidative dehydrogenation process was involved in secondary amine oxidation.

The hydroxalcite-like  $\text{Zn}_6\text{Ti}$ -layered double hydroxide ( $\text{Zn}_6\text{Ti-LDH}$ ) as a doped semiconductor also presented good performance toward imine formation under ultraviolet-light irradiation.<sup>87</sup> The advantages were derived from the enhancement of electron–hole separation by superior dispersion of active  $\text{TiO}_6$  units, and benzylamine and molecular oxygen can independently react with the holes and electrons to form the benzylamine radical cation and superoxide radical anion, respectively. Then, the two radicals reacted together to produce  $\text{H}_2\text{O}_2$  and  $\text{NH}$ -imine intermediates and were further transformed into the desired imines (Scheme 23).

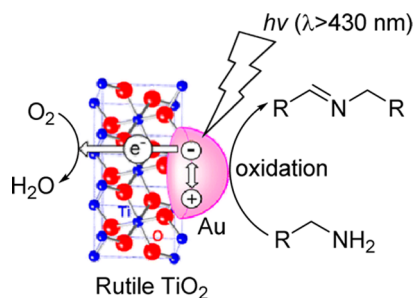
Amine-functionalized Ti-incorporated metal organic framework ( $\text{NH}_2\text{-MIL-125(Ti)}$ ) exhibited good activity for the coupling of benzylamine derivatives under visible-light irradiation.<sup>88</sup> It was demonstrated that the organic linkers in MOF can serve as an antenna to promote electron transfer upon light excitation, and  $\text{TiO}_2$  nanocrystals stabilized by the porous

Scheme 23. Possible Mechanism Catalyzed by Zn<sub>6</sub>Ti-LDH for the Self-Coupling of Benzylamine

inorganic medium can expose more active sites and surface areas to promote the reaction.

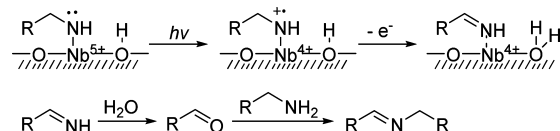
The introduction of noble metals was another strategy to promote the reaction under visible-light irradiation. Tada et al. reported that Au/rutile TiO<sub>2</sub> can catalyze the amine oxidation with high selectivity (>99%) under the light of  $\lambda > 430$  nm and solvent-free conditions.<sup>89</sup> Owing to the localized surface plasmon resonance (LSPR) of Au nanoparticles (NPs), Au/rutile TiO<sub>2</sub> showed a broad ultraviolet–visible absorption, and the intensity could be increased with the Au particle size; however, on the other hand, amines were likely to be adsorbed on the surface of Au NPs than rutile TiO<sub>2</sub>, and small Au NPs would be favorable for this process. Thus, a volcano-shaped curve between the activity and Au particle size was observed with the optimized particle size at 6.7 nm as the balance of LSPR absorption intensity and substrate adsorption. Notably, the excitation of the Au-LSPR rather than the surface complex containing amine was proposed as the driving force for the reaction, and the superiority of Au/rutile TiO<sub>2</sub> to Au/anatase TiO<sub>2</sub> mainly stemmed from the efficiency of electron-transfer from Au NPs to TiO<sub>2</sub>. Therefore, in the anodic process, the LSPR-excited electrons transferring from Au NPs to rutile TiO<sub>2</sub> would lower the Fermi level of Au NPs and enhance the oxidation ability of Au NPs for the oxidation of the adsorbed amines to imines; in the cathodic process, the electrons in the conduction band of rutile TiO<sub>2</sub> were accepted by O<sub>2</sub>, and this process was identified as the rate-determining step of the whole reaction (Scheme 24).

The cross-coupling of benzyl alcohols with anilines was examined by the photocatalyst Au/ZrO<sub>2</sub>, but only 26–62% heterocoupled imines were obtained.<sup>90</sup> Besides, the condensation must be conducted under inert atmosphere since aniline

Scheme 24. Mechanism of Primary Amine Oxidation over Au/TiO<sub>2</sub> Photocatalyst

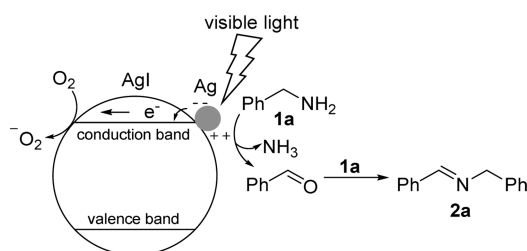
substrates were easily oxidized in the presence of O<sub>2</sub> with visible-light irradiation. Thus, this one-pot, two-step process made the reaction less concise. Shiraishi et al. found the same reaction can be realized in one step with Pt/TiO<sub>2</sub> under N<sub>2</sub> atmosphere.<sup>91</sup> The presence of Pt nanoparticles was proposed to promote the separation of hole–electron pairs generated from TiO<sub>2</sub> under ultraviolet-light irradiation, and alcohols would be subsequently oxidized by the holes to give aldehyde intermediates along with the release of H<sup>+</sup>. Then, the aldehydes were condensed with the amines on the Lewis acid sites of TiO<sub>2</sub> surface to produce imine products. Meanwhile, a portion of the H<sup>+</sup> were reduced by electrons trapped on the Pt particles, but the other portion would react with the surface–OH groups of TiO<sub>2</sub> to form Brønsted acid sites (Ti–OH<sup>2+</sup>), which can protonate amines to reduce their nucleophilicity and were detrimental to the subsequent condensation. Thus, the amount of Pt should be carefully controlled as a higher loading (>0.5 wt %) would result in a large amount of H<sup>+</sup>.

Besides photocatalyst TiO<sub>2</sub>, Tanaka et al. recently investigated various other metal oxide semiconductors and found Nb<sub>2</sub>O<sub>5</sub> was active in amine oxidation.<sup>92</sup> Primary benzylic and aliphatic amines, secondary *N*-alkylbenzylamines, and part of the cyclic amines can be smoothly converted to the target imines in excellent yields under ultraviolet-light irradiation. However, under visible-light irradiation, the oxidation would be less efficient despite the role of the antenna by the substrates. The reaction was proposed to start with the dissociative adsorption of amines to form amide species. Subsequently, the electrons excited from the N 2p orbital of amine species transferred to the conduction band of Nb<sub>2</sub>O<sub>5</sub>, which resulted in the formation of amide radical cations and reduced Nb<sup>4+</sup> simultaneously. Then, the radical cations were further oxidized into NH-imines, and the released electrons were trapped by other Nb<sup>5+</sup> sites. It was worth mentioning that O<sub>2</sub> did not directly participate in amine oxidation but was responsible for the generation of Nb<sup>5+</sup> from the reduced Nb<sup>4+</sup> (Scheme 25).

Scheme 25. Proposed Mechanism Catalyzed by Nb<sub>2</sub>O<sub>5</sub> under Ultraviolet-Light Irradiation

CdS nanosheets<sup>93</sup> and ZnIn<sub>2</sub>S nanospheres<sup>94</sup> were also capable of the self-coupling of benzylamine derivatives under visible-light irradiation. High specific area and unique crystal face exposure were effective ways to improve the catalytic activity of these materials. A similar reaction was investigated by a titanate nanotubes supported AgI (AgI/TNTs) catalyst, and high activity was observed even after filtering out the light of  $\lambda < 490$  nm.<sup>95</sup> Since AgI has a band gap of 2.8 eV and the irradiation with  $\lambda > 443$  nm cannot initiate the photocatalysis reaction, Ag particles generated in situ by partial decomposition of AgI may play an important role in absorbing visible light on account of the LSPR effect. Thus, after transferring the excited electrons to the conduction band of AgI, the formed positively charged Ag nanoparticles were proposed to be responsible for amine oxidation (Scheme 26).

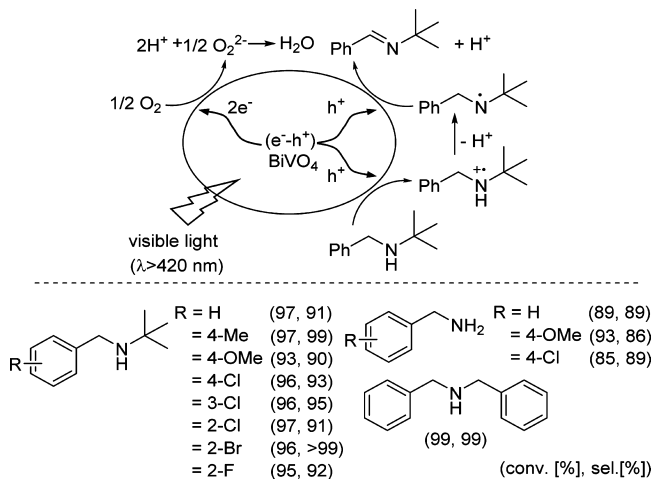
**Scheme 26. Mechanism of Benzylamines Oxidation on AgI/TNTs Photocatalyst**



Cu nanoparticles can also harvest visible-light energy through the LSPR effect, but they were easily oxidized in the presence of O<sub>2</sub>. Quite recently, Guo et al. found Cu nanoparticles can be stabilized using graphene sheets as the support. The prepared Cu/graphene exhibited excellent activity for the coupling of various primary benzylic amines and presented good recyclability in reuse experiments.<sup>96</sup>

Bi-based photocatalysts aimed at the secondary amine oxidation were studied by the Li group. High efficiency was observed for the oxidation of substituted *N*-*t*-butyl and dibenzyl amines with BiVO<sub>4</sub> under visible-light irradiation (Scheme 27).<sup>97</sup> In addition, primary benzylic amines were also suitable for the reaction. It was revealed that the exposure of both (040) and (110) facets of BiVO<sub>4</sub> played important roles in promoting the

**Scheme 27. Proposed Mechanism of Imine Formation Catalyzed by BiVO<sub>4</sub>**



spatial separation of photogenerated electrons and holes to enhance the catalytic activity. Considering the steric hindrance around the nitrogen atom, the adsorption of bulky *N*-*tert*-butyl derivatives on BiVO<sub>4</sub> was unfavorable, and the substrates, therefore, were likely to be oxidized via a direct oxidative dehydrogenation pathway rather than the formation of aldehyde intermediates. Similar results were also obtained employing single-crystalline BiOCl ultrathin nanosheets (BiOCl-UTNSs) as the catalyst,<sup>98</sup> and the high activity was attributed to the enhancement of visible-light absorption by the oxygen vacancies on the (001) facet of BiOCl-UTNSs. Moreover, the oil-compatible and hydrophobic features also affected the finally catalytic efficiency of the material.

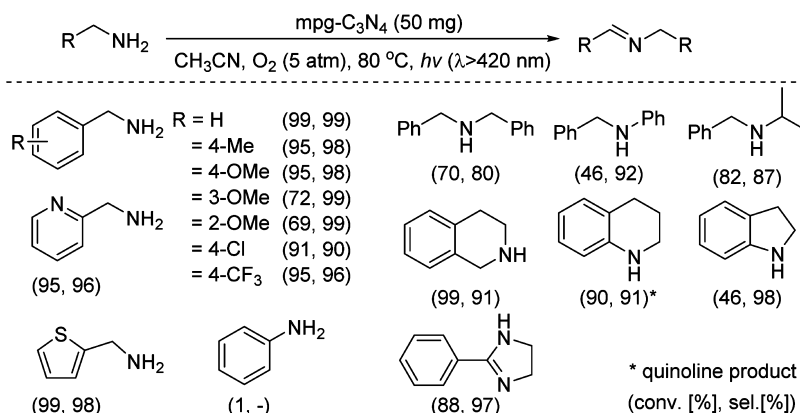
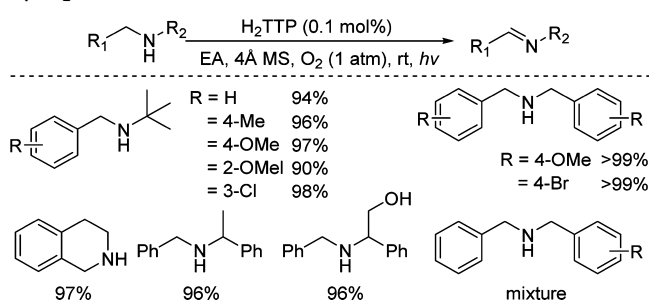
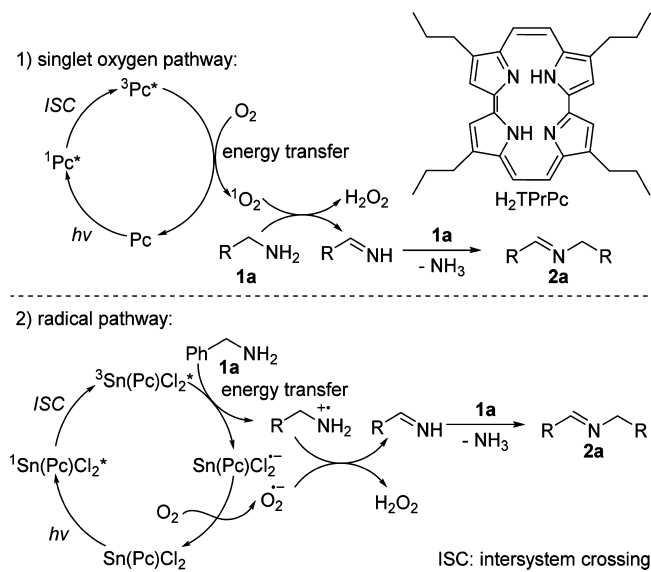
Mesoporous graphite carbon nitride (mpg-C<sub>3</sub>N<sub>4</sub>) as a metal-free photocatalyst presented high activity and selectivity for the oxidation of various primary and secondary amines under visible-light irradiation (Scheme 28).<sup>99</sup> Despite the requirement of a relatively high oxygen pressure and reaction temperature, the imine products can further undergo intramolecular cycloaddition and subsequent oxidation to synthesize benzoxazole, benzimidazole, and benzothiazoles derivatives via a one-pot procedure. The reaction mechanism was similar to that of Zn<sub>6</sub>Ti-LDH system,<sup>87</sup> and the abstraction of proton and hydrogen by superoxide radical anion to form NH-imine intermediate was proposed as the rate-determining step.

**Homogeneous Photocatalytic Systems.** Che et al. showed that singlet oxygen (<sup>1</sup>O<sub>2</sub>) generated from dioxygen by photosensitizer *meso*-tetraphenylporphyrin (H<sub>2</sub>TPP) was capable of the oxidation of secondary amines.<sup>100</sup> The oxidative dehydrogenation selectively occurred at the less-substituted position of branched dibenzylamines, whereas a mixture of four products was obtained for unsymmetric dibenzylamines (Scheme 29), implying an NH-imine hydrolysis/cross-condensation process was involved in the reaction. Besides, the imine products formed in situ can be further applied in Ugi-type reactions via successive condensation with isocyanide and carboxylic acid/nitrophenol. In an extension of this work, the same group found the catalytic efficiency can be greatly improved by employing PdF<sub>20</sub>TPP as the photocatalyst benefiting from the strong absorption in the visible region, long-lived triplet excited states (437 μs), and excellent stability against the oxidative degradation.<sup>101</sup>

Porphycenes, the structural isomers of porphyrins, also showed high activity toward electron-rich benzylamines and secondary amines under visible-light irradiation.<sup>102</sup> Up to 99% imines were obtained within 20 min, but prolonged reaction time or addition of water would result in dominating aldehyde byproducts. Control experiments revealed that the mechanism for 4-methoxybenzylamine oxidation was strongly dependent on the type of photosensitizer. For instance: in the presence of 2,7,12,17-tetrapropylporphycene (H<sub>2</sub>TPrPc), the reaction underwent a singlet oxygen pathway, but in its tin(IV) complex (H<sub>2</sub>TPrPc), a radical pathway was preferred (Scheme 30). It was demonstrated that the redox property of the photocatalyst was an important factor affecting the Gibbs energy of the reaction and thus promoting one of two distinct light-induced oxidation mechanisms.

Bodipy derivatives, possessing strong visible-light absorption and long-lived triplet excited states (1.8–85.2 μs), can efficiently produce singlet oxygen by the triplet-triplet-energy-transfer process and showed high activity toward the oxidation of primary amines and secondary amines.<sup>103</sup> A similar reaction was also investigated by utilizing phenothiazine dyes, and benzylamines



Scheme 28. Oxidation of Various Amines Using mpg-C<sub>3</sub>N<sub>4</sub>Scheme 29. Photochemical Oxidation of Secondary Amines by H<sub>2</sub>TPPScheme 30. Proposed Mechanism of Primary Amine Oxidation Catalyzed by H<sub>2</sub>TPrPc and Sn(TPrPc)Cl<sub>2</sub>

and dibenzylamine can be smoothly oxidized under visible-light irradiation (Scheme 31).<sup>104</sup> It was found the photoactivity of the catalysts were greatly influenced by the substituents attached at the 4-position of the side phenyl groups, and more electron-donating groups were beneficial to stabilize the cationic radical dye species formed in photocatalytic processes.

Transition-metal complexes with photoactivity have also been recently explored for imine formation. Bearing an extended  $\pi$ -conjugated bis-cyclometalated ligand, gold(III) complex (complex A; Scheme 32) with long-lived and highly emissive

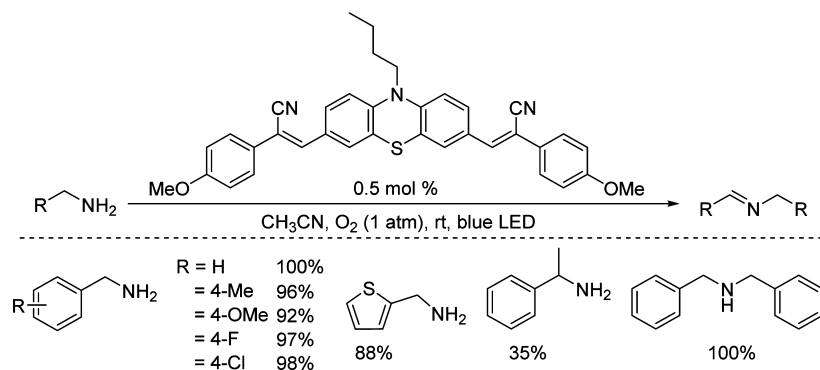
triplet excited states showed high activity for the oxidative dehydrogenation of secondary aromatic amines under visible-light irradiation.<sup>105</sup> Singlet oxygen sensitized from the triplet state of A was suggested to be the active oxidant in the reaction. Similar results were also observed by employing the Pd(II) complex containing a tetradentate  $\text{O}^-\text{N}^-\text{C}^-\text{N}^-\text{O}$  ligand (complex B; Scheme 32).<sup>106</sup>

The self-coupling of primary amines was investigated by Ir(I) complexes (complex C and D; Scheme 32).<sup>107</sup> It was demonstrated that the performance of the catalysts was not only influenced by their optical and electrochemical properties but also by heavy-atom effects. Upon replacing the selenium with sulfur in complex D, the intensity of singlet oxygen was reduced about 41.6%, and the yield of benzylamine oxidation was decreased from 70% to 45%. Besides, photoactive Ru(II) complex with dicarboxylic acid functionality (complex E; Scheme 32) can be further incorporated into a highly stable and porous Zr<sub>6</sub>O<sub>4</sub>(OH)<sub>4</sub>(bpdc)<sub>6</sub> (UiO-67, bpdc = *para*-biphenyl-dicarboxylic acid) framework. The obtained MOF-6 showed comparable activity to the homogeneous complex E but presented good reusability in reuse tests.<sup>108</sup>

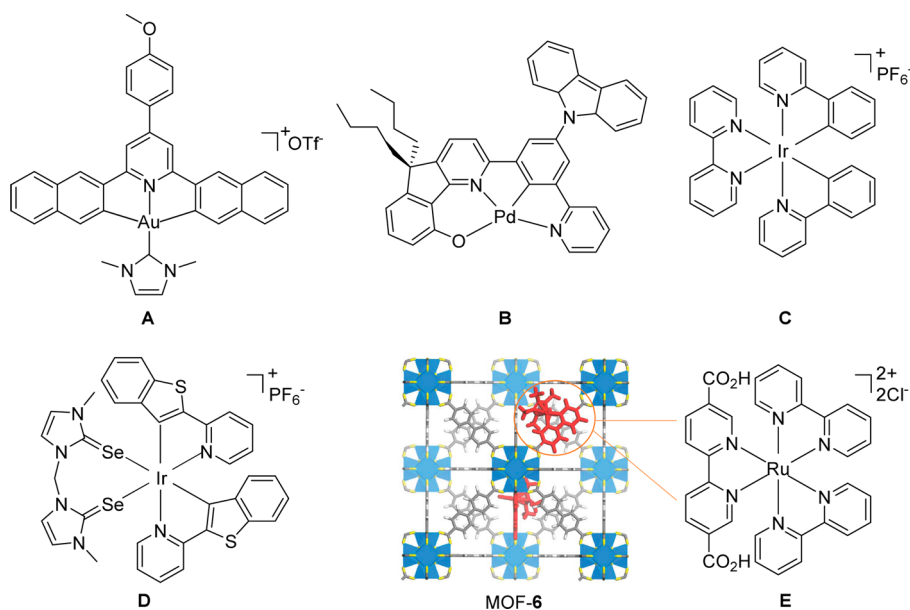
Heterogeneous benzodifuran-containing microporous organic networks (BDF-MON) as a metal-free photocatalyst was also active for the self-coupling of primary amines, and can be reused for several times without loss of activity.<sup>109</sup> Considering the relatively short lifetime of BDF-MON emission (shorter than 5 ns), a radical pathway may be preferred in this catalytic system (Scheme 33).

Given the poor selectivity for the oxidation of unsymmetric secondary amines in many cases, Seeberger et al. recently systemically studied the singlet-oxygen-mediated amine oxidation, and they found that the regioselectivity was strongly influenced by the differences of  $\alpha$ -CH bond hybridization (% s character) and steric factors.<sup>110</sup> As shown in Figure 1, a good linear relationship between the selectivity and the difference in % s character can be established for unsymmetric secondary amines with less bulky substituents (circle dots). The amines with higher differences in % s character gave better selectivity than those with lesser differences, and the oxidative dehydrogenation was preferred to occur at the less-hybridized  $\alpha$ -CH side (Scheme 34a). These intrinsic preferences, however, can be overpowered by the steric factors in some situations (square dots). Fortunately, the deviation of selectivity caused by the steric hindrance was proportionate to conformational free energy of the substituent (A-value) and thus can be well estimated. Notably, this guidance was also suitable for the cross-coupling of

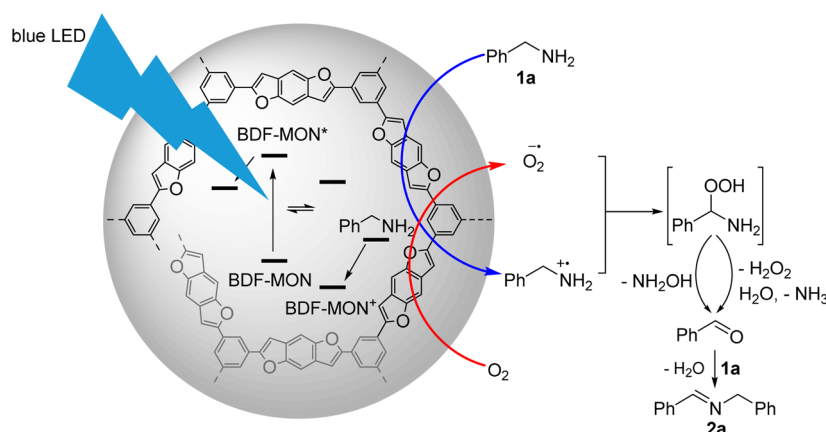
Scheme 31. Photocatalytic Self-Coupling of Amines by Phenothiazine Dyes



Scheme 32. Photocatalytic Amine Oxidation by Various Transition Metal Complexes



Scheme 33. Proposed Photocatalytic Process for the Self-Coupling of Benzylamine by BDF-MON



primary amines. For instance, owing to the same difference in % *s* character, the cross-coupling of 2,6-difluorobenzylamine with an equimolar ratio of benzylamine can give similar selectivity to that observed for the respective secondary amine (Scheme 34a,b). However, it is worth mentioning that the reaction should be first performed at  $-50\text{ }^{\circ}\text{C}$  for generating primary imine and avoiding nucleophilic attack at the same time. As for primary amines

bearing C–H bonds with a similar % *s* character, two independent processes were involved (Scheme 34c).

## 5. BIOINSPIRED CATALYSTS

To make the imine formation more environmentally friendly and efficient, considerable efforts have also been devoted to the design of bioinspired catalysts by simulation of enzymes.<sup>111</sup>

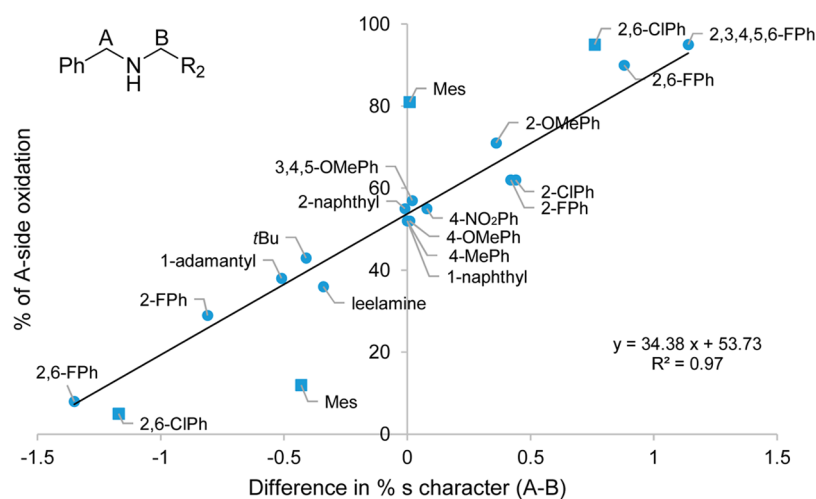
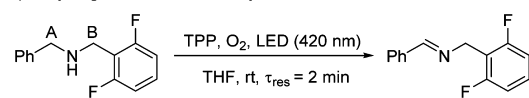


**Figure 1.** Percentage A-side oxidation plotted versus the difference in % s character between the C–H bonds on the A and B sides.

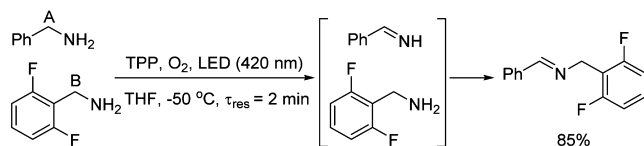
**Scheme 34. Strategies for Imine Synthesis from Secondary or Primary Amines with Different % s Characters (a, b), and from Primary Amines with Similar % s Characters (c)**

a) dehydrogenation of secondary amine with different % s characters



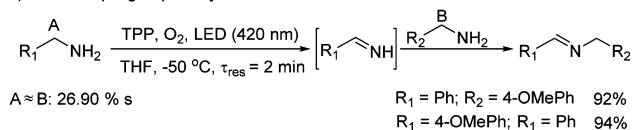
A: 26.90 % s B: 27.78 % s

b) cross-coupling of primary amines with different % s characters



A: 26.90 % s B: 27.78 % s

c) cross-coupling of primary amines with similar % s characters



A ≈ B: 26.90 % s

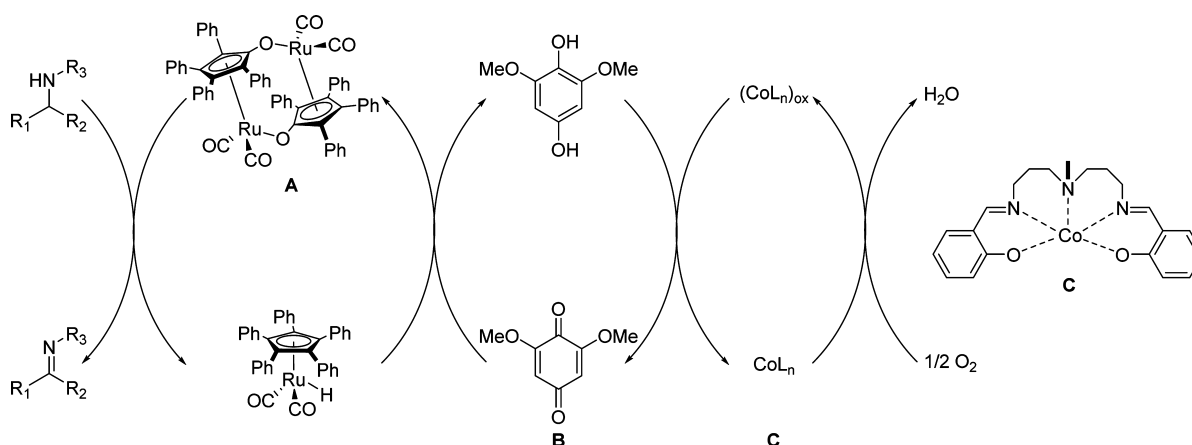
R<sub>1</sub> = Ph; R<sub>2</sub> = 4-OMePh 92%  
R<sub>1</sub> = 4-OMePh; R<sub>2</sub> = Ph 94%

In an early example of this area, Bäckvall et al. reported a ruthenium-based coupled catalytic system for the aerobic oxidation of secondary amines.<sup>112</sup> Binuclear ruthenium complex

A and electron-rich quinone B served as the substrate-selective catalyst and hydrogen acceptor, respectively, and cobalt complex C was responsible for the regeneration of B and the O<sub>2</sub> activation (Scheme 35). Various secondary amines, including  $\alpha$ -branched amines, can be efficiently converted into the corresponding imines with high selectivity. Nevertheless, elevated temperature (110 °C) was required for the reaction to proceed.

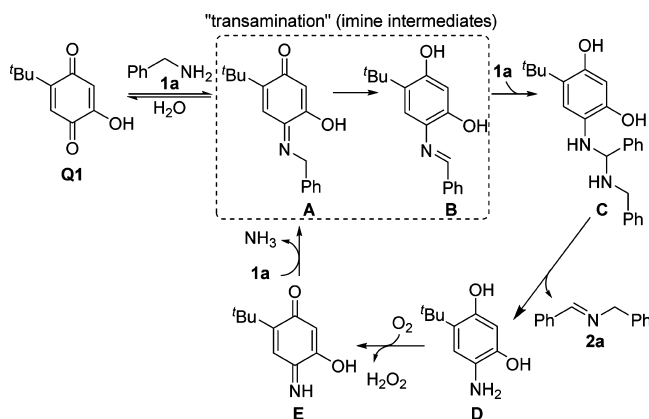
**Quinone-Based Catalysts.** Copper amine oxidases (CuAOs) containing a tyrosine-derived *o*-quinone cofactor in their active site can selectively catalyze the aerobic oxidation of primary amines to aldehydes in natural biological systems.<sup>113</sup> Inspired by this biochemical process, Stahl et al. evaluated the effectiveness of 4-*tert*-butyl-2-hydroxybenzoquinone (TBHBQ, **Q1**) for imine formation in the absence of any additives, and found various benzylamine derivatives can be smoothly self-coupled in acetonitrile at room temperature.<sup>114</sup> A transamination mechanism similar to CuAOs-mediated amine oxidation was proposed: benzylamine was first condensed with **Q1** to form the iminoquinone **A**, and subsequently aromatized to give the highly reactive imine **B**, which resulted in the net two-electron oxidation of the amine and was identified as the rate-limiting step; in organic media, **B** can further react with free benzylamine to generate the aminal **C** rather than hydrolyze into benzyl aldehyde in aqueous solution; after liberating the imine product, **C** was transformed into the reduced aminohydroquinone **D**, followed

**Scheme 35. Proposed Mechanism for Ruthenium-Catalyzed Dehydrogenation of Secondary Amines**



by aerobic oxidation to form the iminoquinone E; finally, E underwent a transamination process with free amine to generate A and close the catalytic cycle (Scheme 36). Given the exquisite

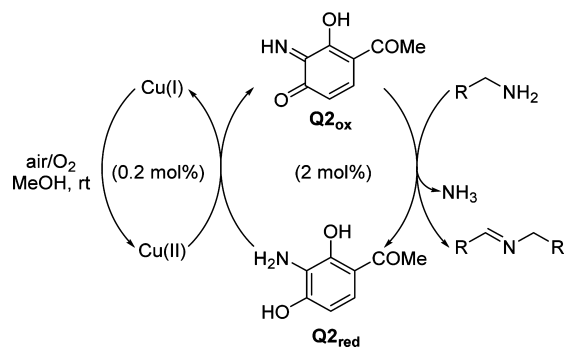
### Scheme 36. Proposed Mechanism of Q1-Mediated Aerobic Oxidation of Primary Amines



formation of homocoupled imines from benzylamines but no activity toward secondary aromatic or aliphatic amines, the preparation of cross-coupled imines, therefore, can be realized by the oxidative self-sorting within dynamic mixtures of homocoupled imines and amines. Experiments revealed the following three factors should be carefully considered to achieve good selectivity: the relative reactivity of two amines toward the oxidation, the relative nucleophilicity of the amines toward the intermediate B, and the equilibrium exchange of the amine substrates with the homocoupled imines.

In the meantime, a Cu<sup>I</sup>/*o*-iminoquinone (Q2<sub>ox</sub>) system for the same reaction was explored by the LARGERON group (Scheme 37).

### Scheme 37. Self-Coupling of Primary Amines Catalyzed by Q2<sub>ox</sub>/Cu<sup>I</sup> Cooperative System



It was found that the generation of Q2<sub>ox</sub> from Q2<sub>red</sub> was very slow under aerobic conditions but can be greatly accelerated by a simple electrolysis procedure or introduction of copper salt as an electron transfer mediator.<sup>115</sup> High performance was achieved for the self-coupling of various primary benzylic amines, and moderate yields were retained for some aliphatic amines.

Quite recently, the same group reported that the homocoupled imine can be further alkylated by a second amine via a transamination process to give the cross-coupled product.<sup>116</sup> Benzylamine derivatives can be selectively coupled with an equimolar ratio of anilines or aliphatic amines under ambient conditions (Scheme 38). Moreover, the cross-coupling of primary aliphatic amines with anilines can also be achieved,

and the obtained aliphatic imines can act in situ as a dienophile for Diels–Alder reactions; however, the coupling of two aliphatic imines was found to be troublesome because of the instability of products.

Utilizing gallacetophenone (THAP) instead of Q2<sub>ox</sub>, the self-coupling of primary amines can also effectively proceed.<sup>117</sup> The presence of organic nanotubes supported gold nanoparticles (AuONT) were responsible for the generation of active *o*-quinone intermediate (X = O) from THAP in the first catalytic cycle and the reoxidation of Q2<sub>red</sub> in subsequent cycles (Scheme 39).

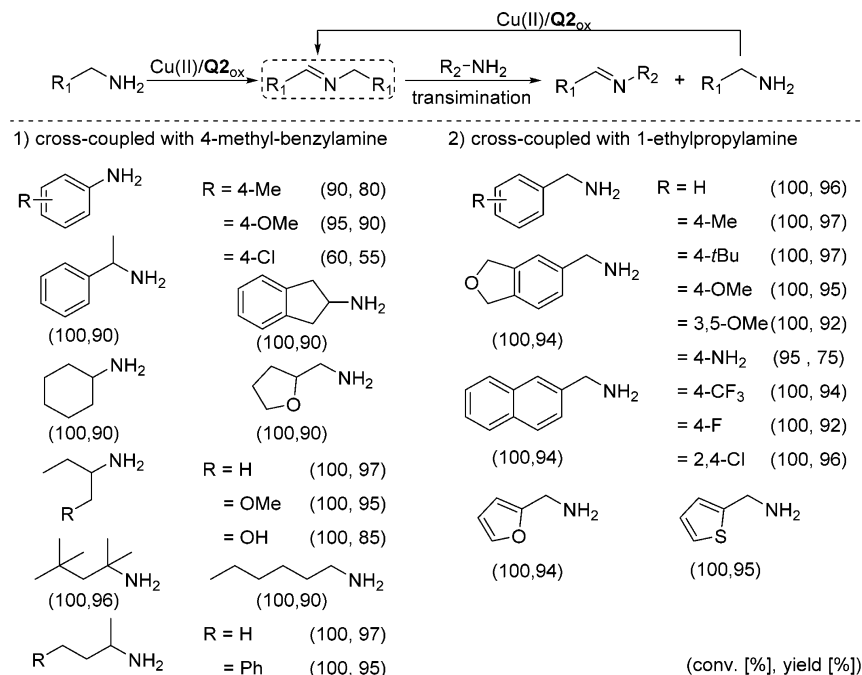
Because Q1 and Q2<sub>ox</sub> mediated amine oxidation via a transamination mechanism, initiated by formation of an imine adduct of the substrate with the quinone, only primary amines can be efficiently transformed into the target imines, and secondary amines were not compatible with this mechanism because they often worked as inhibitors via the formation of irreversible covalent adducts. Nevertheless, quinone cofactors in nature were not restricted to primary amine oxidation. For example, pyrroloquinoline quinone (PQQ)-dependent alcohol dehydrogenases can promote the alcohol oxidation through a hemiacetal intermediate.<sup>118</sup>

On the basis of this information, Stahl et al. reported a new bioinspired quinone catalyst system consisting of 1,10-phenanthroline-5,6-dione (PHD, Q3) and ZnI<sub>2</sub> for the oxidative dehydrogenation of secondary amines.<sup>119</sup> Good to excellent yields were achieved for diverse substrates, ranging from simple dibenzyl amines to different nitrogen heterocycles. It was revealed that the reaction involved an addition–elimination rather than a transamination mechanism (Scheme 40). The introduction of Zn<sup>2+</sup> can enhance the activity of Q3 to significantly accelerate the reaction rate, and the presence of iodide can promote the catalytic turnover by an iodide/triiodide cycle that mediated aerobic reoxidation of PHD-H<sub>2</sub>. In the subsequent work, they further improved the efficiency of this system by replacing Zn<sup>2+</sup> and iodide with Ru<sup>2+</sup> and Co(salophen) (salophen: *N,N'*-bis(salicylidene)-1,2-phenylene-diamine) respectively, and various tetrahydroquinolines can be smoothly transformed into medicinally relevant quinolines under ambient conditions.<sup>120</sup>

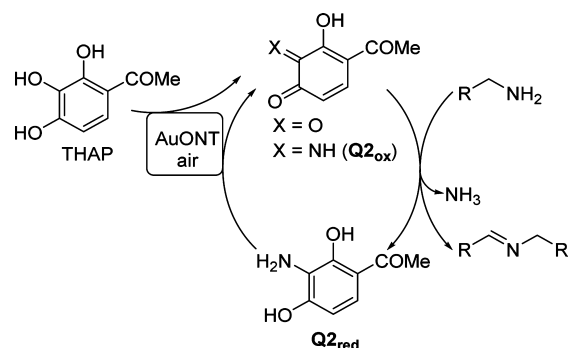
In 2012, Kobayashi et al. discovered a cooperative catalytic system of catechol derivative (Q4<sub>red</sub>) with metal nanoclusters (PI/CB-Pt/Ir: polymer-incarcerated and carbon-stabilized Pt–Ir nanoclusters) for the aerobic oxidation of amines.<sup>121</sup> *O*-quinone B was proposed as the key intermediate by the oxidation of A in the presence of PI/CB-Pt/Ir, which can further react with amine substrates to give the hemiaminals C1 and C2. Notably, different from the above-mentioned transamination (involved in Q1 and Q2) and addition–elimination (involved in Q3) mechanisms, C1 and C2 were complexed to the nanocluster surface, and they underwent hydride transfer and single-electron transfer, respectively, to afford the desired imines (Scheme 41). Therefore, both primary benzylic amines and secondary amines were suitable for this catalytic system, and the supported nanoclusters can be reused up to five times without loss of activity.

Following this work, Doris et al. combined Q4<sub>red</sub> with carbon nanotubes supported rhodium nanoparticles (Ru/CNT) and found it was active toward various N-heterocycle amines under ambient conditions (Scheme 42).<sup>122</sup> Because poor activity was observed upon replacing Q4<sub>red</sub> with 2-*tert*-butylhydroquinone (TBHQ), they believed the catalytic activity of hydroquinone was affected by the geometrical effects of the substituent groups

Scheme 38. Transamination Process for Cross-Coupling of Amines

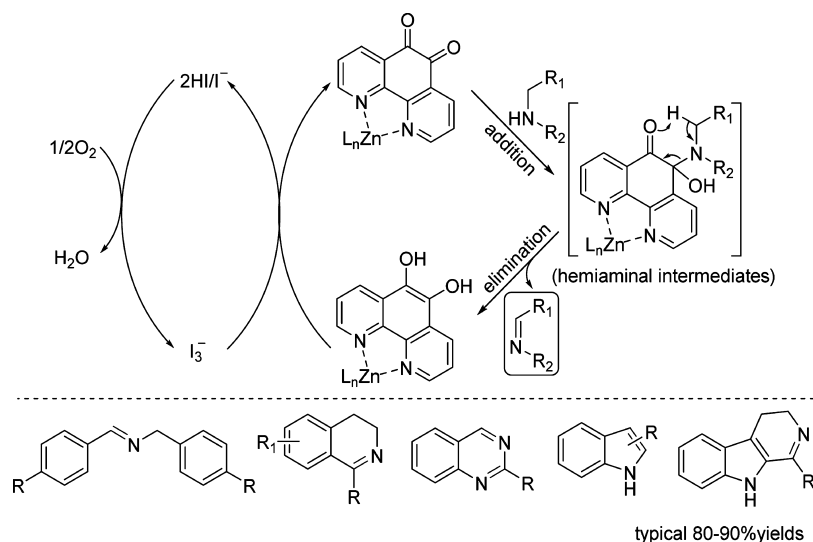


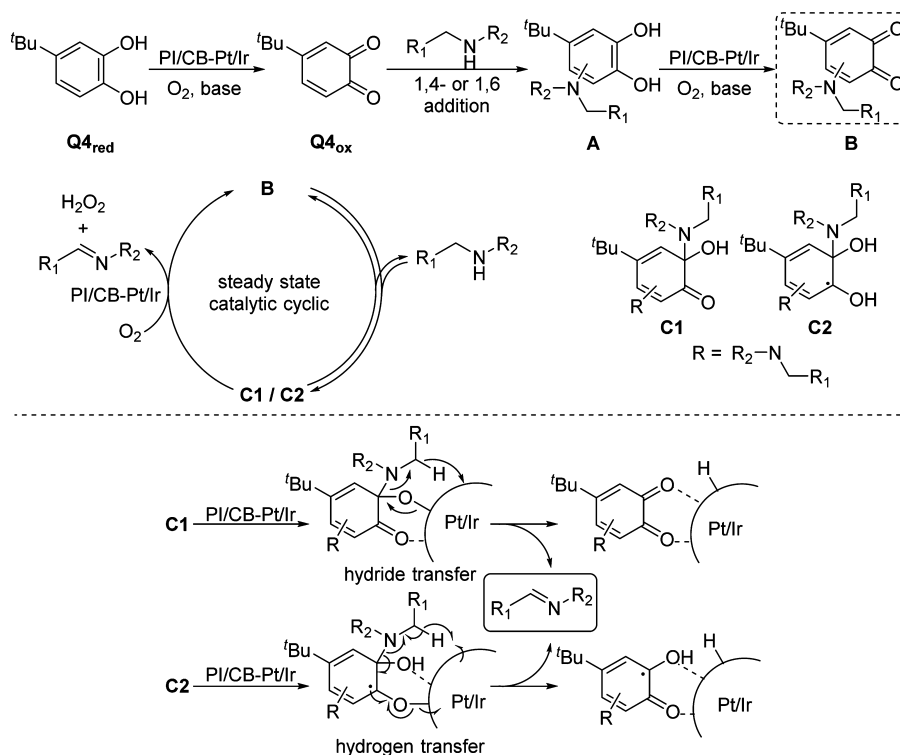
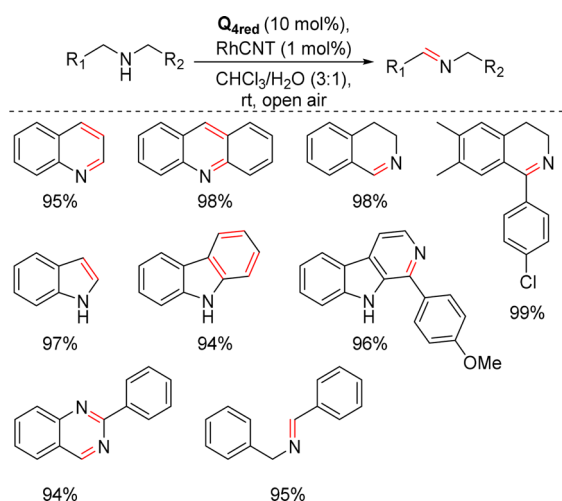
Scheme 39. THAP/AuONT-Catalyzed Imine Formation from Primary Amines



and proposed the addition–elimination mechanism was preferred in this system.

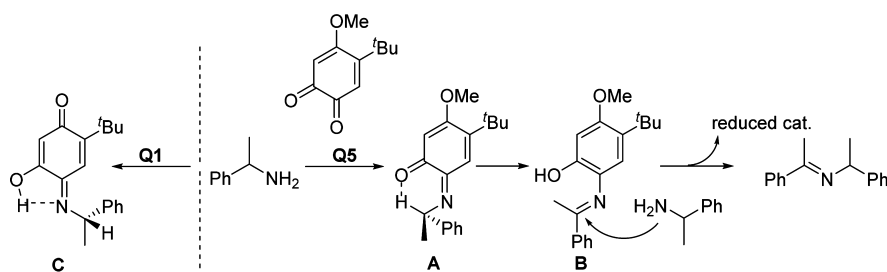
O-quinone **Q5** prepared by modification of **Q4<sub>ox</sub>** with a methoxyl was quite capable of the oxidation of  $\alpha$ -branched primary and cyclic secondary amines in the absence of any metal cocatalyst, whereas **Q4<sub>ox</sub>** itself as well as **Q1** and **Q3** only showed negligible activity under the same conditions.<sup>123</sup> Considering the critical roles of methoxyl, other alkoxy groups such as ethoxyl, iso-propoxyl, and aryloxy were investigated, but the obtained catalysts were less effective, and no activity was observed after removing the *tert*-butyl group of **Q5**. These results strongly revealed that the substituents played vital roles in tuning the activity of **Q5** for amine oxidation and the regeneration of **Q5** by molecular oxygen. The combination of experiments and DFT calculations demonstrated that the reaction involved a transamination mechanism, and the formation of weak C–H...O

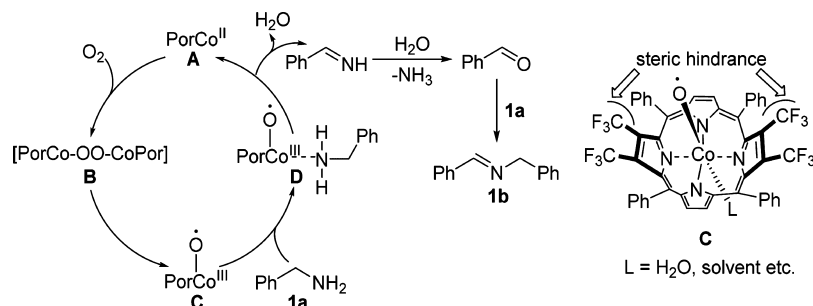
Scheme 40. Mechanism of Secondary Amine Oxidation by **Q3**/ZnI<sub>2</sub>

Scheme 41. Proposed Reaction Mechanisms Mediated by  $Q4_{red}/PICB-Pt/Ir$ Scheme 42. Scopes of  $Q4_{red}/RhCNT$ -Catalyzed Dehydrogenation of Secondary Amines

bond can greatly promote the H-transfer of iminoquinone A to generate the key intermediate B. On the other hand, the strong intramolecular O–H...N bond of intermediate C would hinder the  $\alpha$ -H abstraction, and thus,  $Q1$  was inactive toward the oxidation of  $\alpha$ -branched primary amines (Scheme 43).

**Metalloporphyrin-Based Catalysts.** Metalloporphyrins, as the model of cytochrome P-450, have also been used as bioinspired catalysts for amine oxidation. However, peroxides were often employed as the terminal oxidant.<sup>124</sup> Recently, Chen et al. introduced four trifluoromethyl ( $CF_3$ ) groups into the periphery of porphyrin macrocycle to realize the self-coupling of benzylamines using  $O_2$  as the oxidant.<sup>125</sup> Unlike the quinone-based systems, the reaction mediated by  $CoTPP(CF_3)_4$  was conducted at high temperature (130 °C) and oxygen pressure (6 atm), and prolonged reaction time would result in the decomposition of desired products. The mechanism was proposed as follows: the combination of  $CoTPP(CF_3)_4$  with oxygen would first produce the peroxide B, which was easily decomposed into the key intermediate C; subsequent coordination of benzylamine substrate to C would form the complex D and can be further transformed into NH-imine intermediate; after hydrolysis of this intermediate and condensation with free

Scheme 43. Possible Pathways for the Oxidation of  $\alpha$ -Branched Primary Amines over  $Q5$ 

Scheme 44. Proposed Mechanism of Primary Amine Oxidation Mediated by  $\text{CoTPP}(\text{CF}_3)_4$ 

benzylamine, the imine product was finally obtained (Scheme 44). Owing to the steric hindrance of four  $\text{CF}_3$  groups, the structure of **C** was proposed as a saddle conformation, which can create a cage around the active metal-oxo to prevent the catalyst self-degradation and the formation of an inactive  $\mu$ -oxo dimer. Moreover, the strong electron-withdrawing abilities of the  $\text{CF}_3$  groups can increase the electrophilicity of **C** to further enhanced the catalytic activity.

## 6. CONCLUDING REMARKS

In this review, we have summarized the remarkable achievements that have been made in the formation of imines from alcohols and amines, and four groups of catalysts toward these new approaches using molecular oxygen or air as the terminal oxidant are presented.

- (1) Metal-based catalysts have been greatly explored in both the alcohol and amine oxidation. Homogeneous systems are generally conducted under mild conditions, but extra additives such as ligands and bases are often required. On the other hand, the activity of heterogeneous catalysts strongly depends on the preparations, supports, particle sizes, and interactions between supports and active centers. It is worthy of note that the active sites of a few non-noble metal catalysts are not the metals themselves but the ligands and linkers, and the roles of bases should be carefully evaluated because they not only works as additives but can also catalyze the reaction under specific conditions. Besides, the superiority of noble metal catalysts has not been given full presentation for imine formation; for example, Au-mediated cross-coupling of alcohols with amines often require additional bases, and the oxidation of primary or secondary amines need prolonged times and high temperatures.
- (2) Metal-free catalysts have been successfully applied to the oxidation of amines but not yet for the cross-coupling of alcohols with amines. The preparations and treatments greatly affect the finally activity of carbon-based catalysts, and the formations of hydrogen bonds with substrates are crucial for water and ionic liquids-mediated reactions. The mechanisms in homogeneous systems are well clarified, whereas the active sites of heterogeneous carbon materials are still unclear in many cases; however, promising results have been achieved.
- (3) Similar to metal-free catalysts, photocatalysts have been mainly studied in amine oxidation. By introducing metal nanoparticles, doping a secondary element, exposing specific facets, solid semiconductors present appreciable activity under the visible-light region. Besides, high performance is also achieved with photoactive organic

complexes and porous polymers, and singlet oxygen and radical mechanisms are proposed on the basis of the properties of the catalysts. Moreover, valuable guidance for the oxidation of unsymmetric secondary amines and the cross-coupling of two different amines will make the imine formation more selective and efficient.

- (4) Bioinspired catalysts have received particular attention owing to their high activity and selectivity under mild conditions. Five types of quinones aiming at different amine substrates have been greatly studied, and the corresponding mechanisms including transamination, addition–elimination, hydride transfer, and single-electron transfer have also been proposed. Moreover, benzylamine derivatives can be selectively coupled with anilines or aliphatic amines via a transamination process, which provides a good alternative to the cross-coupling of alcohols with amines for the preparation of heterocoupled imines. The activity of these systems is strongly influenced not only by quinones themselves but also by the additional promoters, especially noble metal cocatalysts. Besides, other classes of bioinspired catalysts are far from development to date.

Although it is still a long way to achieve the practical synthesis of imines from alcohols and amines, there have been exciting results. Developments emerging from quinone-based biomimetic systems (**Q1** ~ **Q5**), non-noble catalysts like versatile  $\text{Fe}(\text{NO}_3)_2/\text{TEMPO}$ , high-activity  $\text{CeO}_2$ , Al-based MOF-253, and carbon-based materials bring great hope and inspiration to this goal. We believe that the development of new multifunctional high-activity catalysts, exploration of reaction mechanisms, and green synthesis will continue to be the core topics of imine formation, and we sincerely hope this review can serve as a useful reference for chemists dedicating to this area and inspire more creative work to flourish these new approaches.

## AUTHOR INFORMATION

### Corresponding Author

\*E-mail: [sgao@dicp.ac.cn](mailto:sgao@dicp.ac.cn).

### Notes

The authors declare no competing financial interest.

## ACKNOWLEDGMENTS

We gratefully acknowledge financial support from the National Natural Science Foundation of China (21403219) and National Engineering Laboratory for Methanol to Olefins.

## REFERENCES

- (1) (a) Murahashi, S. I. *Angew. Chem., Int. Ed. Engl.* **1995**, *34*, 2443–2465. (b) Yao, S.; Saaby, S.; Hazell, R. G.; Jorgensen, K. A. *Chem. - Eur. J.*

- 2000, 6, 2435–2448. (c) Liu, Z.-Y.; Wang, Y.-M.; Li, Z.-R.; Jiang, J.-D.; Boykin, D. W. *Bioorg. Med. Chem. Lett.* **2009**, 19, 5661–5664.
- (2) (a) Kobayashi, S.; Ishitani, H. *Chem. Rev.* **1999**, 99, 1069–1094. (b) Adams, J. P. J. *Chem. Soc., Perkin Trans. 1* **2000**, 2, 125–139. (c) Chen, D.; Wang, Y.; Klankermayer, J. *Angew. Chem., Int. Ed.* **2010**, 49, 9475–9478. (d) Kobayashi, S.; Mori, Y.; Fossey, J. S.; Salter, M. M. *Chem. Rev.* **2011**, 111, 2626–2704. (e) He, R.; Jin, X.; Chen, H.; Huang, Z.-T.; Zheng, Q.-Y.; Wang, C. *J. Am. Chem. Soc.* **2014**, 136, 6558–6561. (f) Kondo, M.; Kobayashi, N.; Hatanaka, T.; Funahashi, Y.; Nakamura, S. *Chem. - Eur. J.* **2015**, 21, 9066–9070.
- (3) (a) Schiff, H. *Justus Liebigs Ann. Chem.* **1864**, 131, 118–119. (b) Westheimer, F.; Taguchi, K. *J. Org. Chem.* **1971**, 36, 1570–1572. (c) Varma, R. S.; Dahiya, R.; Kumar, S. *Tetrahedron Lett.* **1997**, 38, 2039–2042. (d) Liu, G.; Cogan, D. A.; Owens, T. D.; Tang, T. P.; Ellman, J. A. *J. Org. Chem.* **1999**, 64, 1278–1284. (e) Naeimi, H.; Salimi, F.; Rabiei, K. *J. Mol. Catal. A: Chem.* **2006**, 260, 100–104. (f) Reeves, J. T.; Visco, M. D.; Marsini, M. A.; Grinberg, N.; Busacca, C. A.; Mattson, A. E.; Senanayake, C. H. *Org. Lett.* **2015**, 17, 2442–2445.
- (4) (a) Schümperli, M. T.; Hammond, C.; Hermans, I. *ACS Catal.* **2012**, 2, 1108–1117. (b) LARGERON, M. *Eur. J. Org. Chem.* **2013**, 2013, 5225–5235. (c) Qin, W.; Long, S.; Panunzio, M.; Biondi, S. *Molecules* **2013**, 18, 12264–12289. (d) Patil, R. D.; Adimurthy, S. *Asian J. Org. Chem.* **2013**, 2, 726–744. (e) Yadav, D. K. T.; Bhanage, B. M. *RSC Adv.* **2015**, 5, 12387–12391.
- (5) Kopylovich, M. N.; Ribeiro, A. P.; Alegria, E. C.; Martins, N. M.; Martins, L. M.; Pombeiro, A. J. *Adv. Organomet. Chem.* **2015**, 63, 91–174.
- (6) (a) Yamaguchi, R.; Ikeda, C.; Takahashi, Y.; Fujita, K.-i. *J. Am. Chem. Soc.* **2009**, 131, 8410–8412. (b) Xu, C.; Goh, L. Y.; Pullarkat, S. A. *Organometallics* **2011**, 30, 6499–6502. (c) Ho, H.-A.; Manna, K.; Sadow, A. D. *Angew. Chem., Int. Ed.* **2012**, 51, 8607–8610. (d) Gnanaprakasam, B.; Zhang, J.; Milstein, D. *Angew. Chem., Int. Ed.* **2010**, 49, 1468–1471. (e) Maggi, A.; Madsen, R. *Organometallics* **2012**, 31, 451–455. (f) Li, H.; Wang, X.; Wen, M.; Wang, Z.-X. *Eur. J. Inorg. Chem.* **2012**, 2012, 5011–5020. (g) Rigoli, J. W.; Moyer, S. A.; Pearce, S. D.; Schomaker, J. M. *Org. Biomol. Chem.* **2012**, 10, 1746–1749. (h) Balaraman, E.; Srimani, D.; Diskin-Posner, Y.; Milstein, D. *Catal. Lett.* **2015**, 145, 139–144. (i) Sindhuja, E.; Ramesh, R. *Tetrahedron Lett.* **2014**, 55, 5504–5507. (j) Saha, B.; Wahidur Rahaman, S. M.; Daw, P.; Sengupta, G.; Bera, J. K. *Chem. - Eur. J.* **2014**, 20, 6542–6551.
- (7) (a) Guillena, G.; Ramón, D. J.; Yus, M. *Chem. Rev.* **2010**, 110, 1611–1641. (b) Yang, Q.; Wang, Q.; Yu, Z. *Chem. Soc. Rev.* **2015**, 44, 2305–2329.
- (8) Patil, R. D.; Adimurthy, S. *Adv. Synth. Catal.* **2011**, 353, 1695–1700.
- (9) Patil, R. D.; Adimurthy, S. *RSC Adv.* **2012**, 2, 5119–5122.
- (10) Wang, J.; Lu, S.; Cao, X.; Gu, H. *Chem. Commun.* **2014**, 50, 5637–5640.
- (11) Kang, Q.; Zhang, Y. *Green Chem.* **2012**, 14, 1016–1019.
- (12) Lan, Y.-S.; Liao, B.-S.; Liu, Y.-H.; Peng, S.-M.; Liu, S.-T. *Eur. J. Org. Chem.* **2013**, 2013, 5160–5164.
- (13) Hu, Z.; Kerton, F. M. *Org. Biomol. Chem.* **2012**, 10, 1618–1624.
- (14) Huang, B.; Tian, H.; Lin, S.; Xie, M.; Yu, X.; Xu, Q. *Tetrahedron Lett.* **2013**, 54, 2861–2864.
- (15) Sonobe, T.; Oisaki, K.; Kanai, M. *Chem. Sci.* **2012**, 3, 3249–3255.
- (16) Ryland, B. L.; Stahl, S. S. *Angew. Chem., Int. Ed.* **2014**, 53, 8824–8838.
- (17) Tian, H.; Yu, X.; Li, Q.; Wang, J.; Xu, Q. *Adv. Synth. Catal.* **2012**, 354, 2671–2677.
- (18) Guan, M.; Wang, C.; Zhang, J.; Zhao, Y. *RSC Adv.* **2014**, 4, 48777–48782.
- (19) Al-Hmoud, L.; Jones, C. W. *J. Catal.* **2013**, 301, 116–124.
- (20) Pérez, J. M.; Cano, R.; Yus, M.; Ramón, D. J. *Eur. J. Org. Chem.* **2012**, 2012, 4548–4554.
- (21) Bai, L.; Dang, Z. *RSC Adv.* **2015**, 5, 10341–10345.
- (22) Zhang, E.; Tian, H.; Xu, S.; Yu, X.; Xu, Q. *Org. Lett.* **2013**, 15, 2704–2707.
- (23) Khusnutdinov, R. I.; Baygusina, A. R.; Aminov, R. I. *Russ. J. Org. Chem.* **2012**, 48, 1059–1061.
- (24) Huo, C.; Xie, H.; Wu, M.; Jia, X.; Wang, X.; Chen, F.; Tang, J. *Chem. - Eur. J.* **2015**, 21, 5723–5726.
- (25) Dhakshinamoorthy, A.; Alvaro, M.; Garcia, H. *ChemCatChem* **2010**, 2, 1438–1443.
- (26) Qiu, X.; Len, C.; Luque, R.; Li, Y. *ChemSusChem* **2014**, 7, 1684–1688.
- (27) Tayade, K. N.; Mishra, M. *J. Mol. Catal. A: Chem.* **2014**, 382, 114–125.
- (28) Kodama, S.; Yoshida, J.; Nomoto, A.; Ueta, Y.; Yano, S.; Ueshima, M.; Ogawa, A. *Tetrahedron Lett.* **2010**, 51, 2450–2452.
- (29) Wang, L.; Chen, B.; Ren, L.; Zhang, H.; Lü, Y.; Gao, S. *Chin. J. Catal.* **2015**, 36, 19–23.
- (30) Rao, K. T. V.; Haribabu, B.; Prasad, P. S. S.; Lingaiah, N. *Green Chem.* **2013**, 15, 837–846.
- (31) Chu, G.; Li, C. *Org. Biomol. Chem.* **2010**, 8, 4716–4719.
- (32) Tamura, M.; Tomishige, K. *Angew. Chem., Int. Ed.* **2015**, 54, 864–867.
- (33) Zhang, Z.; Wang, Y.; Wang, M.; Lu, J.; Li, L.; Zhang, Z.; Li, M.; Jiang, J.; Wang, F. *Chin. J. Catal.* **2015**, 36, DOI: 10.1016/S1872-2067(15)60869-5.
- (34) Sudarsanam, P.; Rangaswamy, A.; Reddy, B. M. *RSC Adv.* **2014**, 4, 46378–46382.
- (35) Govinda Rao, B.; Sudarsanam, P.; Rangaswamy, A.; Reddy, B. M. *Catal. Lett.* **2015**, 145, 1436–1445.
- (36) Ahmad, S.; Gopalaiiah, K.; Chandrudu, S. N.; Nagarajan, R. *Inorg. Chem.* **2014**, 53, 2030–2039.
- (37) (a) Sithambaram, S.; Kumar, R.; Son, Y.-C.; Suib, S. L. *J. Catal.* **2008**, 253, 269–277. (b) Makwana, V. D.; Son, Y.-C.; Howell, A. R.; Suib, S. L. *J. Catal.* **2002**, 210, 46–52.
- (38) Chen, B.; Li, J.; Dai, W.; Wang, L.; Gao, S. *Green Chem.* **2014**, 16, 3328.
- (39) Wang, Y.; Kobayashi, H.; Yamaguchi, K.; Mizuno, N. *Chem. Commun.* **2012**, 48, 2642.
- (40) Zhang, Z.; Wang, F.; Wang, M.; Xu, S.; Chen, H.; Zhang, C.; Xu, J. *Green Chem.* **2014**, 16, 2523.
- (41) Biswas, S.; Dutta, B.; Mullick, K.; Kuo, C.-H.; Poyraz, A. S.; Suib, S. L. *ACS Catal.* **2015**, 5, 4394–4403.
- (42) Jiang, L.; Jin, L.; Tian, H.; Yuan, X.; Yu, X.; Xu, Q. *Chem. Commun.* **2011**, 47, 10833–10835.
- (43) Kwon, M. S.; Kim, S.; Park, S.; Bosco, W.; Chidrala, R. K.; Park, J. *J. Org. Chem.* **2009**, 74, 2877–2879.
- (44) Cui, W.; Zhaorigetu, B.; Jia, M.; Ao, W.; Zhu, H. *RSC Adv.* **2014**, 4, 2601–2604.
- (45) (a) Furukawa, S.; Suga, A.; Komatsu, T. *Chem. Commun.* **2014**, 50, 3277–3280. (b) Furukawa, S.; Suga, A.; Komatsu, T. *ACS Catal.* **2015**, 5, 1214–1222.
- (46) Zhu, B.; Angelici, R. J. *Chem. Commun.* **2007**, 21, 2157–2159.
- (47) Zhu, B.; Lazar, M.; Trewyn, B. G.; Angelici, R. J. *J. Catal.* **2008**, 260, 1–6.
- (48) Aschwanden, L.; Mallat, T.; Grunwaldt, J.-D.; Krumeich, F.; Baiker, A. *J. Mol. Catal. A: Chem.* **2009**, 300, 111–115.
- (49) Aschwanden, L.; Mallat, T.; Krumeich, F.; Baiker, A. *J. Mol. Catal. A: Chem.* **2009**, 309, 57–62.
- (50) Aschwanden, L.; Mallat, T.; Maciejewski, M.; Krumeich, F.; Baiker, A. *ChemCatChem* **2010**, 2, 666–673.
- (51) Aschwanden, L.; Panella, B.; Rossbach, P.; Keller, B.; Baiker, A. *ChemCatChem* **2009**, 1, 111–115.
- (52) Grirrane, A.; Corma, A.; Garcia, H. *J. Catal.* **2009**, 264, 138–144.
- (53) Miyamura, H.; Morita, M.; Inasaki, T.; Kobayashi, S. *Bull. Chem. Soc. Jpn.* **2011**, 84, 588–599.
- (54) Sudarsanam, P.; Selvakannan, P. R.; Soni, S. K.; Bhargava, S. K.; Reddy, B. M. *RSC Adv.* **2014**, 4, 43460–43469.
- (55) Oprea, C. M.; Pavel, O. D.; Moragues, A.; El Haskourib, J.; Beltrán, D.; Amorós, P.; Marcos, M. D.; Stoflea, L. E.; Parvulescu, V. I. *Catal. Sci. Technol.* **2014**, 4, 4340–4355.
- (56) Wang, M.; Wang, F.; Ma, J.; Li, M.; Zhang, Z.; Wang, Y.; Zhang, X.; Xu, J. *Chem. Commun.* **2013**, 50, 292–294.
- (57) So, M.-H.; Liu, Y.; Ho, C.-M.; Che, C.-M. *Chem. - Asian J.* **2009**, 4, 1551–1561.



- (58) (a) Amaya, T.; Ito, T.; Inada, Y.; Saio, D.; Hirao, T. *Tetrahedron Lett.* **2012**, *53*, 6144–6147. (b) Amaya, T.; Ito, T.; Hirao, T. *Tetrahedron Lett.* **2013**, *54*, 2409–2411.
- (59) (a) Neeli, C. K. P.; Ravi Kumar, M.; Saidulu, G.; Rama Rao, K. S.; Burri, D. R. *J. Chem. Technol. Biotechnol.* **2015**, *90*, 1657–1664. (b) Neeli, C. K. P.; Ganji, S.; Ganjala, V. S. P.; Kamaraju, S. R. R.; Burri, D. R. *RSC Adv.* **2014**, *4*, 14128.
- (60) Guo, H.; Kemell, M.; Al-Hunaiti, A.; Rautiainen, S.; Leskelä, M.; Repo, T. *Catal. Commun.* **2011**, *12*, 1260–1264.
- (61) Sun, H.; Su, F.-Z.; Ni, J.; Cao, Y.; He, H.-Y.; Fan, K.-N. *Angew. Chem., Int. Ed.* **2009**, *48*, 4390–4393.
- (62) Liu, P.; Li, C.; Hensen, E. J. M. *Chem. - Eur. J.* **2012**, *18*, 12122–12129.
- (63) Kegnæs, S.; Mielby, J.; Mentzel, U. V.; Christensen, C. H.; Riisager, A. *Green Chem.* **2010**, *12*, 1437–1441.
- (64) Cui, W.; Zhu, H.; Jia, M.; Ao, W.; Zhang, Y.; Zhaorigetu, B. *React. Kinet., Mech. Catal.* **2013**, *109*, 551–562.
- (65) Cui, W.; Xiao, Q.; Sarina, S.; Ao, W.; Xie, M.; Zhu, H.; Bao, Z. *Catal. Today* **2014**, *235*, 152–159.
- (66) Soulé, J.-F.; Miyamura, H.; Kobayashi, S. *Chem. Commun.* **2012**, *49*, 355–357.
- (67) Zhang, L.; Wang, W.; Wang, A.; Cui, Y.; Yang, X.; Huang, Y.; Liu, X.; Liu, W.; Son, J.-Y.; Oji, H.; Zhang, T. *Green Chem.* **2013**, *15*, 2680–2684.
- (68) (a) Mielby, J.; Poreddy, R.; Engelbrekt, C.; Kegnæs, S. *Chin. J. Catal.* **2014**, *35*, 670–676. (b) Poreddy, R.; García-Suárez, E. J.; Riisager, A.; Kegnæs, S. *Dalton Trans.* **2014**, *43*, 4255–4259.
- (69) Han, L.; Xing, P.; Jiang, B. *Org. Lett.* **2014**, *16*, 3428–3431.
- (70) Hammond, C.; Schümperli, M. T.; Hermans, I. *Chem. - Eur. J.* **2013**, *19*, 13193–13198.
- (71) Kim, J. W.; He, J.; Yamaguchi, K.; Mizuno, N. *Chem. Lett.* **2009**, *38*, 920–921.
- (72) Cano, R.; Ramon, D. J.; Yus, M. *J. Org. Chem.* **2011**, *76*, 5547–5557.
- (73) He, W.; Wang, L.; Sun, C.; Wu, K.; He, S.; Chen, J.; Wu, P.; Yu, Z. *Chem. - Eur. J.* **2011**, *17*, 13308–13317.
- (74) Xu, J.; Zhuang, R.; Bao, L.; Tang, G.; Zhao, Y. *Green Chem.* **2012**, *14*, 2384–2387.
- (75) Donthiri, R. R.; Patil, R. D.; Adimurthy, S. *Eur. J. Org. Chem.* **2012**, *2012*, 4457–4460.
- (76) Huang, H.; Huang, J.; Liu, Y.-M.; He, H.-Y.; Cao, Y.; Fan, K.-N. *Green Chem.* **2012**, *14*, 930–934.
- (77) Su, C.; Acik, M.; Takai, K.; Lu, J.; Hao, S.-j.; Zheng, Y.; Wu, P.; Bao, Q.; Enoki, T.; Chabal, Y. J.; Ping Loh, K. *Nat. Commun.* **2012**, *3*, 1298.
- (78) Li, X.-H.; Antonietti, M. *Angew. Chem., Int. Ed.* **2013**, *52*, 4572–4576.
- (79) Wang, H.; Zheng, X.; Chen, H.; Yan, K.; Zhu, Z.; Yang, S. *Chem. Commun.* **2014**, *50*, 7517–7520.
- (80) Chen, B.; Wang, L.; Dai, W.; Shang, S.; Lv, Y.; Gao, S. *ACS Catal.* **2015**, *5*, 2788–2794.
- (81) Liu, L.; Zhang, S.; Fu, X.; Yan, C.-H. *Chem. Commun.* **2011**, *47*, 10148–10150.
- (82) Monopoli, A.; Cotugno, P.; Iannone, F.; Ciminale, F.; Dell'Anna, M. M.; Mastroilli, P.; Nacci, A. *Eur. J. Org. Chem.* **2014**, *2014*, 5925–5931.
- (83) Liu, L.; Wang, Z.; Fu, X.; Yan, C.-H. *Org. Lett.* **2012**, *14*, 5692–5695.
- (84) (a) Lang, X.; Ma, W.; Chen, C.; Ji, H.; Zhao, J. *Acc. Chem. Res.* **2013**, *47*, 355–363. (b) Lang, X.; Chen, X.; Zhao, J. *Chem. Soc. Rev.* **2014**, *43*, 473–486.
- (85) (a) Lang, X.; Ji, H.; Chen, C.; Ma, W.; Zhao, J. *Angew. Chem., Int. Ed.* **2011**, *50*, 3934–3937. (b) Li, N.; Lang, X.; Ma, W.; Ji, H.; Chen, C.; Zhao, J. *Chem. Commun.* **2013**, *49*, 5034–5036.
- (86) Lang, X.; Ma, W.; Zhao, Y.; Chen, C.; Ji, H.; Zhao, J. *Chem. - Eur. J.* **2012**, *18*, 2624–2631.
- (87) Yang, X.-J.; Chen, B.; Li, X.-B.; Zheng, L.-Q.; Wu, L.-Z.; Tung, C.-H. *Chem. Commun.* **2014**, *50*, 6664–6667.
- (88) Sun, D.; Ye, L.; Li, Z. *Appl. Catal., B* **2015**, *164*, 428–432.
- (89) Naya, S.-i.; Kimura, K.; Tada, H. *ACS Catal.* **2013**, *3*, 10–13.
- (90) Zheng, J.; Li, J.; Wei, H.; Yu, J.; Su, H.; Wang, X. *Mater. Sci. Semicond. Process.* **2015**, *32*, 131–136.
- (91) (a) Shiraiishi, Y.; Fujiwara, K.; Sugano, Y.; Ichikawa, S.; Hirai, T. *ACS Catal.* **2013**, *3*, 312–320. (b) Shiraiishi, Y.; Ikeda, M.; Tsukamoto, D.; Tanaka, S.; Hirai, T. *Chem. Commun.* **2011**, *47*, 4811–4813.
- (92) Furukawa, S.; Ohno, Y.; Shishido, T.; Teramura, K.; Tanaka, T. *ACS Catal.* **2011**, *1*, 1150–1153.
- (93) Zhao, W.; Liu, C.; Cao, L.; Yin, X.; Xu, H.; Zhang, B. *RSC Adv.* **2013**, *3*, 22944–22948.
- (94) Ye, L.; Li, Z. *ChemCatChem* **2014**, *6*, 2540–2543.
- (95) Zheng, Z.; Chen, C.; Bo, A.; Zavahir, F. S.; Waclawik, E. R.; Zhao, J.; Yang, D.; Zhu, H. *ChemCatChem* **2014**, *6*, 1210–1214.
- (96) Zhai, Z.; Guo, X.; Jin, G.; Guo, X.-Y. *Catal. Sci. Technol.* **2015**, *5*, 4202–4207.
- (97) Yuan, B.; Chong, R.; Zhang, B.; Li, J.; Liu, Y.; Li, C. *Chem. Commun.* **2014**, *50*, 15593–15596.
- (98) Wu, Y. H.; Yuan, B.; Li, M. R.; Zhang, W. H.; Liu, Y.; Li, C. *Chem. Sci.* **2015**, *6*, 1873–1878.
- (99) Su, F.; Mathew, S. C.; Möhlmann, L.; Antonietti, M.; Wang, X.; Blechert, S. *Angew. Chem., Int. Ed.* **2011**, *50*, 657–660.
- (100) Jiang, G.; Chen, J.; Huang, J.-S.; Che, C.-M. *Org. Lett.* **2009**, *11*, 4568–4571.
- (101) To, W.-P.; Liu, Y.; Lau, T.-C.; Che, C.-M. *Chem. - Eur. J.* **2013**, *19*, 5654–5664.
- (102) Berlicka, A.; König, B. *Photochem. Photobiol. Sci.* **2010**, *9*, 1359–1366.
- (103) (a) Huang, L.; Zhao, J.; Guo, S.; Zhang, C.; Ma, J. *J. Org. Chem.* **2013**, *78*, 5627–5637. (b) Zhou, Y.; Zhou, Z.; Li, Y.; Yang, W. *Catal. Commun.* **2015**, *64*, 96–100.
- (104) Park, J. H.; Ko, K. C.; Kim, E.; Park, N.; Ko, J. H.; Ryu, D. H.; Ahn, T. K.; Lee, J. Y.; Son, S. U. *Org. Lett.* **2012**, *14*, 5502–5505.
- (105) To, W.-P.; Tong, G. S.-M.; Lu, W.; Ma, C.; Liu, J.; Chow, A. L.-F.; Che, C.-M. *Angew. Chem., Int. Ed.* **2012**, *51*, 2654–2657.
- (106) Chow, P. K.; Ma, C.; To, W.-P.; Tong, G. S. M.; Lai, S.-L.; Kui, S. C. F.; Kwok, W.-M.; Che, C.-M. *Angew. Chem., Int. Ed.* **2013**, *52*, 11775–11779.
- (107) (a) Rueping, M.; Vila, C.; Szadkowska, A.; Koenigs, R. M.; Fronert, J. *ACS Catal.* **2012**, *2*, 2810–2815. (b) Jin, J.; Shin, H.-W.; Park, J. H.; Park, J. H.; Kim, E.; Ahn, T. K.; Ryu, D. H.; Son, S. U. *Organometallics* **2013**, *32*, 3954–3959.
- (108) Wang, C.; Xie, Z.; deKrafft, K. E.; Lin, W. *J. Am. Chem. Soc.* **2011**, *133*, 13445–13454.
- (109) Kang, N.; Park, J. H.; Ko, K. C.; Chun, J.; Kim, E.; Shin, H.-W.; Lee, S. M.; Kim, H. J.; Ahn, T. K.; Lee, J. Y.; Son, S. U. *Angew. Chem., Int. Ed.* **2013**, *52*, 6228–6232.
- (110) Ushakov, D. B.; Plutschack, M. B.; Gilmore, K.; Seeberger, P. H. *Chem. - Eur. J.* **2015**, *21*, 6528–6534.
- (111) Largeron, M.; Fleury, M.-B. *Science* **2013**, *339*, 43–44.
- (112) (a) Samec, J. S.; Éll, A. H.; Bäckvall, J. E. *Chem. - Eur. J.* **2005**, *11*, 2327–2334. (b) Ibrahim, I.; Samec, J. S.; Bäckvall, J. E.; Córdova, A. *Tetrahedron Lett.* **2005**, *46*, 3965–3968. (c) Piera, J.; Bäckvall, J. E. *Angew. Chem., Int. Ed.* **2008**, *47*, 3506–3523.
- (113) Mure, M. *Acc. Chem. Res.* **2004**, *37*, 131–139.
- (114) Wendlandt, A. E.; Stahl, S. S. *Org. Lett.* **2012**, *14*, 2850–2853.
- (115) (a) Largeron, M.; Chiaroni, A.; Fleury, M. B. *Chem. - Eur. J.* **2008**, *14*, 996–1003. (b) Largeron, M.; Fleury, M. B. *Angew. Chem., Int. Ed.* **2012**, *51*, 5409–5412.
- (116) Largeron, M.; Fleury, M.-B. *Chem. - Eur. J.* **2015**, *21*, 3815–3820.
- (117) Jawale, D. V.; Gravel, E.; Villemain, E.; Shah, N.; Geertsen, V.; Namboothiri, I. N. N.; Doris, E. *Chem. Commun.* **2014**, *50*, 15251–15254.
- (118) (a) Itoh, S.; Kawakami, H.; Fukuzumi, S. *J. Am. Chem. Soc.* **1997**, *119*, 439–440. (b) Itoh, S.; Kawakami, H.; Fukuzumi, S. *Biochemistry* **1998**, *37*, 6562–6571.
- (119) Wendlandt, A. E.; Stahl, S. S. *J. Am. Chem. Soc.* **2014**, *136*, 506–512.
- (120) Wendlandt, A. E.; Stahl, S. S. *J. Am. Chem. Soc.* **2014**, *136*, 11910–11913.

- (121) Yuan, H.; Yoo, W.-J.; Miyamura, H.; Kobayashi, S. *J. Am. Chem. Soc.* **2012**, *134*, 13970–13973.
- (122) Jawale, D. V.; Gravel, E.; Shah, N.; Dauvois, V.; Li, H.; Namboothiri, I. N. N.; Doris, E. *Chem. - Eur. J.* **2015**, *21*, 7039–7042.
- (123) Qin, Y.; Zhang, L.; Lv, J.; Luo, S.; Cheng, J.-P. *Org. Lett.* **2015**, *17*, 1469–1472.
- (124) (a) Maruyama, K.; Kusakawa, T.; Higuchi, Y.; Nishinaga, A. *Stud. Surf. Sci. Catal.* **1991**, *66*, 489–495. (b) Yuan, Q.-L.; Zhou, X.-T.; Ji, H.-B. *Catal. Commun.* **2010**, *12*, 202–206. (c) Zhou, X.-T.; Ren, Q.-G.; Ji, H.-B. *Tetrahedron Lett.* **2012**, *53*, 3369–3373.
- (125) Zhao, S.; Liu, C.; Guo, Y.; Xiao, J.-C.; Chen, Q.-Y. *J. Org. Chem.* **2014**, *79*, 8926–8931.